

## RESEARCH ARTICLE

# Wnt/ $\beta$ -catenin signaling via Axin2 is required for myogenesis and, together with YAP/Taz and Tead1, active in Ila/Iix muscle fibers

Danyil Huraskin<sup>1,‡</sup>, Nane Eiber<sup>1,‡</sup>, Martin Reichel<sup>2,\*</sup>, Laura M. Zidek<sup>3</sup>, Bojana Kravic<sup>1</sup>, Dominic Bernkopf<sup>2</sup>, Julia von Maltzahn<sup>3</sup>, Jürgen Behrens<sup>2</sup> and Said Hashemolhosseini<sup>1,¶</sup>

**ABSTRACT**

Canonical Wnt/ $\beta$ -catenin signaling plays an important role in myogenic differentiation, but its physiological role in muscle fibers remains elusive. Here, we studied activation of Wnt/ $\beta$ -catenin signaling in adult muscle fibers and muscle stem cells in an Axin2 reporter mouse. Axin2 is a negative regulator and a target of Wnt/ $\beta$ -catenin signaling. In adult muscle fibers, Wnt/ $\beta$ -catenin signaling is only detectable in a subset of fast fibers that have a significantly smaller diameter than other fast fibers. In the same fibers, immunofluorescence staining for YAP/Taz and Tead1 was detected. Wnt/ $\beta$ -catenin signaling was absent in quiescent and activated satellite cells. Upon injury, Wnt/ $\beta$ -catenin signaling was detected in muscle fibers with centrally located nuclei. During differentiation of myoblasts expression of Axin2, but not of Axin1, increased together with Tead1 target gene expression. Furthermore, absence of Axin1 and Axin2 interfered with myoblast proliferation and myotube formation, respectively. Treatment with the canonical Wnt3a ligand also inhibited myotube formation. Wnt3a activated TOPflash and Tead1 reporter activity, whereas neither reporter was activated in the presence of Dkk1, an inhibitor of canonical Wnt signaling. We propose that Axin2-dependent Wnt/ $\beta$ -catenin signaling is involved in myotube formation and, together with YAP/Taz/Tead1, associated with reduced muscle fiber diameter of a subset of fast fibers.

**KEY WORDS:** Axin2, Yap1, Wwtr1, Tead1, Skeletal muscle, Muscle fibers, Satellite cells

**INTRODUCTION**

The Wnt gene family encodes 19 secreted glycoproteins, which bind to the Frizzled (Fzd) transmembrane receptors on target cells. Wnt proteins regulate key processes such as development and differentiation (Bhanot et al., 1996; Cadigan and Nusse, 1997; Clevers, 2006; von Maltzahn et al., 2012) and are fundamental during embryonic myogenesis (von Maltzahn et al., 2012). For instance, they regulate the development of embryonic muscle in a spatiotemporal manner. Wnt1, Wnt3a and Wnt4 are expressed in the dorsal regions of the neural tube, whereas Wnt4, Wnt6 and Wnt7a

are expressed in the dorsal ectoderm, and Wnt11 is expressed in the epaxial dermomyotome. In adult muscle, Wnt proteins are expressed upon regeneration (Poleskaya et al., 2003; von Maltzahn et al., 2012). Non-canonical Wnt signaling through Wnt7a regulates satellite cell number and the size of skeletal muscle (Le Grand et al., 2009; von Maltzahn et al., 2013). Generally, non-canonical Wnt signaling is required for skeletal muscle development, while canonical Wnt signaling, especially via Wnt3a, has been demonstrated to lead to increased fibrosis (Brack et al., 2007).

In canonical Wnt signaling the Wnt binds to the Fzd and Lrp5/6 receptor pairs, thereby leading to the inactivation of glycogen synthase kinase 3 $\beta$  (GSK3 $\beta$ ) through dishevelled (Dsh). In the absence of Wnt stimulation,  $\beta$ -catenin forms a destruction complex with adenomatous polyposis coli (APC), Axin1 and GSK3 $\beta$  (MacDonald et al., 2009). Phosphorylation of  $\beta$ -catenin by casein kinase I (CK1) and GSK3 $\beta$  causes ubiquitylation and proteasome-mediated degradation of  $\beta$ -catenin. The presence of Wnt ligand results in the activation of Dsh, which leads to phosphorylation-dependent recruitment of Axin1 to the low-density lipoprotein receptor-related protein (LRP) receptor and disassembly of the  $\beta$ -catenin degradation complex. Stabilized  $\beta$ -catenin accumulates in the cytoplasm and translocates to the nucleus. There, it complexes with T cell factor/lymphoid enhancer factor (TCF/LEF) transcription factors and acts as a transcriptional coactivator to induce the context-dependent expression of Wnt/ $\beta$ -catenin target genes (Eastman and Grosschedl, 1999). In contrast to canonical Wnt signaling, non-canonical Wnt signaling does not require the activity of  $\beta$ -catenin. Examples of non-canonical Wnt signaling pathways in skeletal muscle are the planar cell polarity (PCP) and the AKT/mTOR (Bentzinger et al., 2014; Le Grand et al., 2009; von Maltzahn et al., 2013) pathways.

Mechanical load or training can lead to an increase of myofiber size, accompanied by muscle enlargement. This condition is called hypertrophy and multiple studies identified different roles for canonical and non-canonical Wnt signaling in muscle fiber hypertrophy (Armstrong and Esser, 2005; Bernardi et al., 2011; Han et al., 2011; Rochat et al., 2004; von Maltzahn et al., 2011). Furthermore, expression of  $\beta$ -catenin is a prerequisite for the physiological growth of adult skeletal muscle, underscoring the importance of canonical Wnt signaling (Armstrong et al., 2006). A recent study employed TCF reporter mice to gain further insights into the role of canonical Wnt signaling (Kuroda et al., 2013). They found that canonical Wnt signaling is strongly activated during fetal myogenesis and only weakly activated in adult muscles, where it is limited to slow myofibers. Their data suggest that canonical Wnt signaling promotes the formation of, or switch to, slow fiber types and inhibits myogenesis (Kuroda et al., 2013). Furthermore, they demonstrated that Wnt1 and Wnt3a are potent activators of canonical Wnt signaling in myogenic progenitors using a TCF-luciferase reporter assay.

<sup>1</sup>Institute of Biochemistry, Fahrstrasse 17, Friedrich-Alexander University Erlangen-Nürnberg, Erlangen D-91054, Germany. <sup>2</sup>Nikolaus-Fiebiger-Center of Molecular Medicine, Glückstrasse 6, Friedrich-Alexander University Erlangen-Nürnberg, Erlangen D-91054, Germany. <sup>3</sup>Leibniz Institute for Age Research/Fritz Lipmann Institute (FLI), Beutenbergstrasse 11, Jena D-07745, Germany.

\*Present address: Department of Psychiatry and Psychotherapy, Schwabachanlage 6, Friedrich-Alexander University Erlangen-Nürnberg, Erlangen D-91054, Germany.

<sup>‡</sup>These authors contributed equally to this work

<sup>¶</sup>Author for correspondence (said.hashemolhosseini@fau.de)

 S.H., 0000-0002-6564-5649

Axin1 and Axin2 are closely related (~45% amino acid identity) negative regulators of canonical Wnt signaling (Behrens et al., 1998; Zeng et al., 1997). They have similar biochemical and cell biological properties but may differ in their *in vivo* functions. Whereas Axin1 is homogeneously distributed in the mouse embryo (Zeng et al., 1997), *Axin2* is a Wnt target gene and more selectively expressed in specific tissues (Behrens et al., 1998). Mutant embryos lacking Axin1 die at embryonic day (E) 9.5, with abnormalities including truncation of the forebrain, neural tube defects and embryonic axis duplications (Gluecksohn-Schoenheimer, 1949; Perry et al., 1995). Mice lacking Axin2 are viable but display craniofacial defects (Lustig et al., 2002; Yu et al., 2005). Interestingly, Axin2 has been shown to be upregulated in C2C12 mouse myoblast cells during differentiation (Bernardi et al., 2011; Figeac and Zammit, 2015). Importantly, no *in vivo* data on the function of Axin2 in skeletal muscle are available so far.

Another important pathway involved in the control of organ size, tissue regeneration and stem cell self-renewal is the Hippo pathway (Zhao et al., 2011). In mammals, the activation of kinases MST1/2 (also known as Stk4/3; homologs of *Drosophila* Hippo) and LATS1/2 leads to LATS-dependent phosphorylation of Taz (also known as Wwtr1) and YAP (also known as Yap1), thereby decreasing their stability, nuclear localization and transcriptional activity (Pan, 2010). Recently, YAP was identified as a crucial regulator of muscle fiber size (Watt et al., 2015). Moreover, YAP/Taz are incorporated into the  $\beta$ -catenin destruction complex and, thereby, orchestrate the Wnt response (Azzolin et al., 2014, 2012).

Here, we elucidated the role of canonical Wnt signaling activity in adult muscle fibers using a well-established *Axin2-lacZ* reporter mouse paradigm (Lustig et al., 2002). In these mice, canonical Wnt signaling is reflected by *lacZ* expression under control of the endogenous *Axin2* promoter. We detected active canonical Wnt signaling (1) in myotubes derived from cultured C2C12 cells or murine primary myoblasts, (2) in muscle fibers of type IIa and, most likely, type IIx, (3) at neuromuscular synapses and (4) during regeneration of skeletal muscle after injury. Interestingly, YAP/Taz/Tead1-mediated signaling accompanied canonical Wnt signaling in adult muscle fibers.  $\beta$ -galactosidase-positive muscle fibers (reflecting canonical Wnt activity) were also positive for  $\beta$ -catenin, YAP/Taz and Tead1. In cultured muscle cells (1) the absence of Axin1 interfered with proliferation, (2) the absence of Axin2 slowed down differentiation into myotubes and treatment with Wnt3a had a similar effect, and (3) after knockdown of  $\beta$ -catenin or Tead1 myogenesis was increased. Moreover, canonical Wnt3a induced TOPflash and Tead1 reporters and, importantly, neither induction occurred in the presence of Dkk1, an inhibitor of canonical Wnt signaling.

## RESULTS

### Axin2 expression and canonical Wnt signaling are induced in cultured muscle cells during differentiation

Wnt signaling plays a crucial and complex role in myogenesis (von Maltzahn et al., 2012). We were interested in the biological role of Axin1 and Axin2, as negative regulators of canonical Wnt signaling, in muscle cells and analyzed their expression in cultured C2C12 cells, a well-established *in vitro* muscle differentiation paradigm that recapitulates myogenic differentiation (Blau et al., 1983). *In situ* hybridizations were performed for *Axin1* and *Axin2* transcripts in proliferating myoblasts and differentiating myotubes (Fig. 1A). *Axin1* mRNA was detected in myoblasts and myotubes, while *Axin2* was mainly found in myoblasts with extended processes and, even more

prominently, in multi-nucleated myotubes (Fig. 1A). To follow the temporal expression profile and protein expression of Axin1 and Axin2, proliferating C2C12 myoblasts and differentiating myotubes were analyzed by immunoblot. Axin1 appeared to be constitutively expressed, whereas Axin2 protein was not detectable in myoblasts but increased gradually in differentiating myotubes (Fig. 1B,C). Expression of *Axin1* and *Axin2* in C2C12 cells was validated by quantitative PCR analysis (Fig. 1D). A TOPflash assay showed an increase in  $\beta$ -catenin/TCF-mediated gene transcription upon differentiation (Fig. 1E). Altogether, Axin2 expression and  $\beta$ -catenin-mediated canonical Wnt activity increased in differentiating myotubes.

### Expression profile of Axin2 in adult skeletal muscles

The importance of canonical Wnt/ $\beta$ -catenin signaling in resting adult myofibers *in vivo* is not known. Therefore, we investigated the expression profile of Axin2 (using *Axin2-lacZ* mice) as a reporter for canonical Wnt signaling in different adult skeletal muscles. In *Axin2-lacZ* mice, the *lacZ* cassette is inserted in frame with the ATG start codon of *Axin2* and thus  $\beta$ -galactosidase ( $\beta$ -gal) activity reflects *Axin2* gene expression (Lustig et al., 2002). Diaphragm muscles of *Axin2-lacZ* reporter mice were dissected and stained with X-Gal (Fig. 2A). As expected, myofibers of diaphragms of wild-type littermates did not show any positive staining even after 24 h of incubation with X-Gal, whereas many myofibers of heterozygous *Axin2-lacZ* diaphragm muscles already turned blue after 4 h (Fig. 2A). Additionally, some blue spots appeared on the heterozygous *Axin2-lacZ* diaphragms, preferentially at the endplate zone, and were associated with neuromuscular synapses (Fig. 2A,B). After 1.5 h of staining, reporter expression was significantly higher in homozygous *Axin2-lacZ* diaphragms than in heterozygous diaphragms after 4 h of staining, indicating that the absence of Axin2 relieved the repression of  $\beta$ -catenin/TCF-mediated gene transcription (Fig. 2A).

Intriguingly, in the heterozygous and homozygous *Axin2-lacZ* diaphragms, canonical Wnt signaling was turned on only in a subset of muscle fibers (Fig. 2A). To understand whether there are muscle-specific differences regarding canonical Wnt signaling, X-Gal staining was performed on transverse sections of different hindlimb muscles. In heterozygous *Axin2-lacZ* mice, the most prominent  $\beta$ -gal-positive fibers appeared in the plantaris muscle and the extensor digitorum longus (Fig. 2C–F). In homozygous *Axin2-lacZ* muscles, positively stained fibers were apparent in most analyzed muscles of the calf and shinbone (Fig. 2D). Almost no staining was detected in the soleus muscle (Fig. 2D). Whereas transverse sections of heterozygous tibialis anterior muscle showed weak blue staining, homozygous *Axin2-lacZ* muscle fibers exhibited intense blue staining (Fig. 2F). Quantitative PCR analysis was performed with cDNAs of five different wild-type muscles to analyze endogenous *Axin2* mRNA levels (Fig. 2G). In agreement with the results obtained by X-Gal staining using *Axin2-lacZ* reporter mice (Fig. 2A,D,F), the *Axin2* transcript level was lowest in the soleus muscle (Fig. 2G).

To understand whether the higher  $\beta$ -gal activity in homozygous *Axin2-lacZ* muscles reflects a gene dosage effect, or is the consequence of stronger induction of canonical Wnt signaling activity due to absence of the negative regulator Axin2, we quantified the amount of  $\beta$ -gal protein in heterozygous and homozygous *Axin2-lacZ* muscles. In homozygous muscles,  $\beta$ -gal levels were 5-fold higher in diaphragm and 10-fold higher in the tibialis anterior muscle than in heterozygous muscles of the same type (Fig. 2H,I), clearly pointing to a  $\beta$ -catenin-mediated increase of reporter *Axin2-lacZ* expression rather than a gene dosage effect.

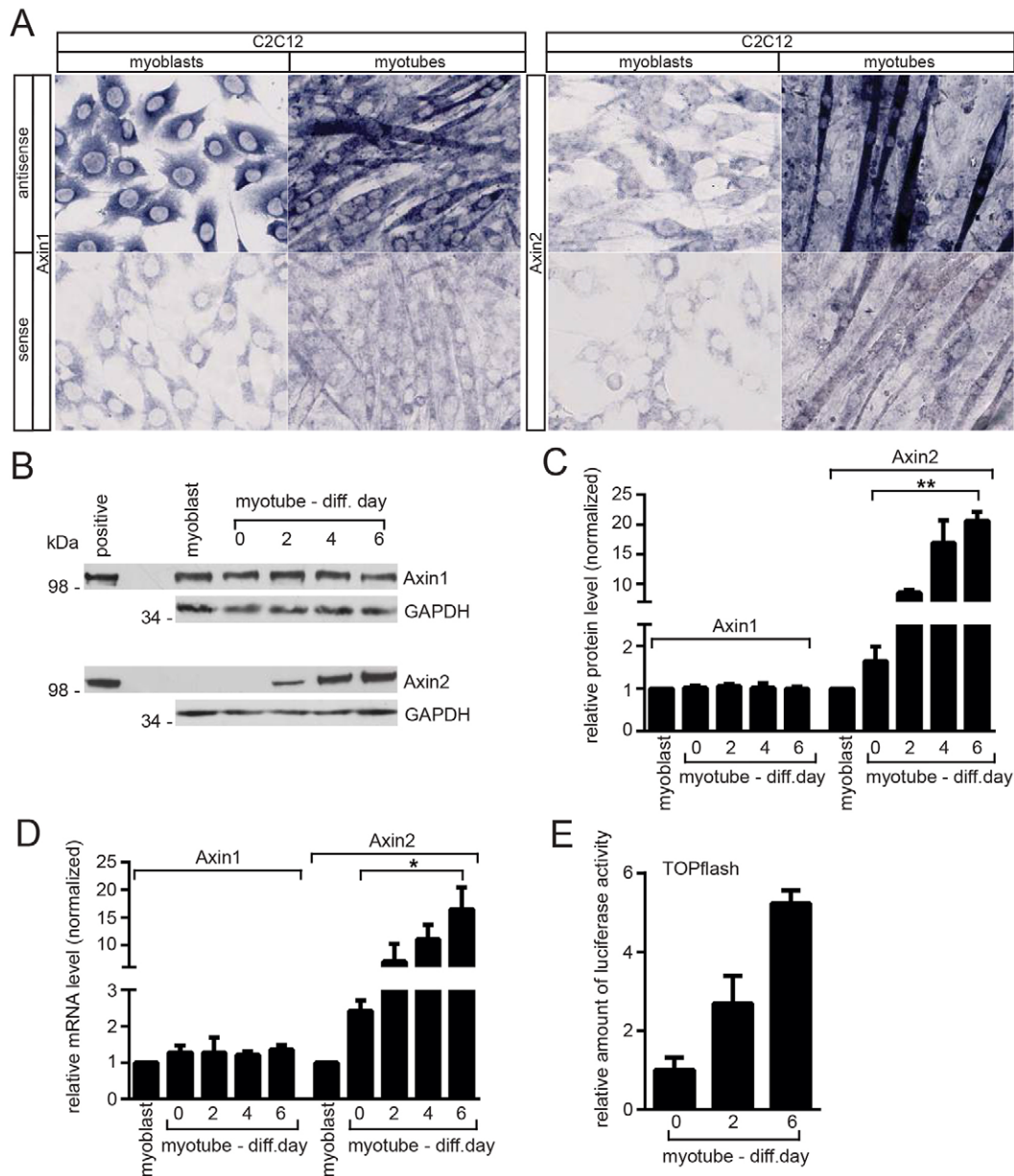


**Fig. 1. Expression of axins and canonical Wnt signaling in muscle cells.** (A) *In situ* hybridization was performed with C2C12 myoblast and myotube cultures and *in situ* probes specific for *Axin1* or *Axin2*. Although *Axin1* transcription is similar in myoblasts and myotubes, *Axin2* staining is drastically increased in myotubes compared with myoblasts. (B) Western blot showing expression of *Axin1* and *Axin2* using lysates from C2C12 myoblasts or myotubes at the indicated days of culture. *Axin1* was present in all samples, whereas *Axin2* is induced during differentiation from myoblasts to myotubes. (C) Quantification of *Axin1* and *Axin2* protein levels as shown in B.  $n=3$  sets of cells. (D) Relative transcript levels for *Axin1* and *Axin2* in differentiating C2C12 cells as determined by quantitative PCR.  $n=3$  sets of cells and 3 qPCR runs for each set of cells. (E) After transfection of C2C12 muscle cells with TOPflash reporter, cell extracts were prepared at the indicated days of differentiation for luciferase assay.  $n=5$  sets of cells, each as duplicate.  $*P<0.05$ ,  $**P<0.01$  (unpaired two-tailed *t*-test). Error bars represent s.d.

### Muscle fibers expressing *Axin2-lacZ* are type IIa and, most likely, type IIx

In order to determine which types of muscle fibers were  $\beta$ -gal positive, a series of co-stainings for  $\beta$ -gal and myosin heavy chain (MyHC) markers were performed using antibodies with specificities for fiber types I, IIa, and IIb. Any type II fibers that were not stained by fiber type IIa-specific or IIb-specific antibodies were considered to be type IIx. We analyzed four muscle types: (1) the plantaris muscle, which contains blue-stained fibers in heterozygotes and homozygotes and is mainly composed of type IIa, IIb and IIx fibers (Agbulut et al., 2003); (2) the extensor digitorum longus, which is mainly composed of type II fibers and

also contains intensely stained fibers in heterozygotes and homozygotes; (3) the tibialis anterior, which contains mostly weakly stained fibers in heterozygotes (Fig. 2F); and (4) the gastrocnemius medialis, which contains type II and slow type I fibers.

In plantaris muscles from *Axin2-lacZ* mice almost all  $\beta$ -gal-positive fibers were also positive for MyHC type IIa but not IIb (Fig. 3A,C). The remaining  $\beta$ -gal-positive fibers are therefore most likely type IIx (Fig. 3C). We found a similar distribution of  $\beta$ -gal-expressing fast fiber types in the extensor digitorum longus and tibialis anterior, as that observed in the plantaris (Fig. 3A,C). We asked whether type I fibers might also be  $\beta$ -gal positive and

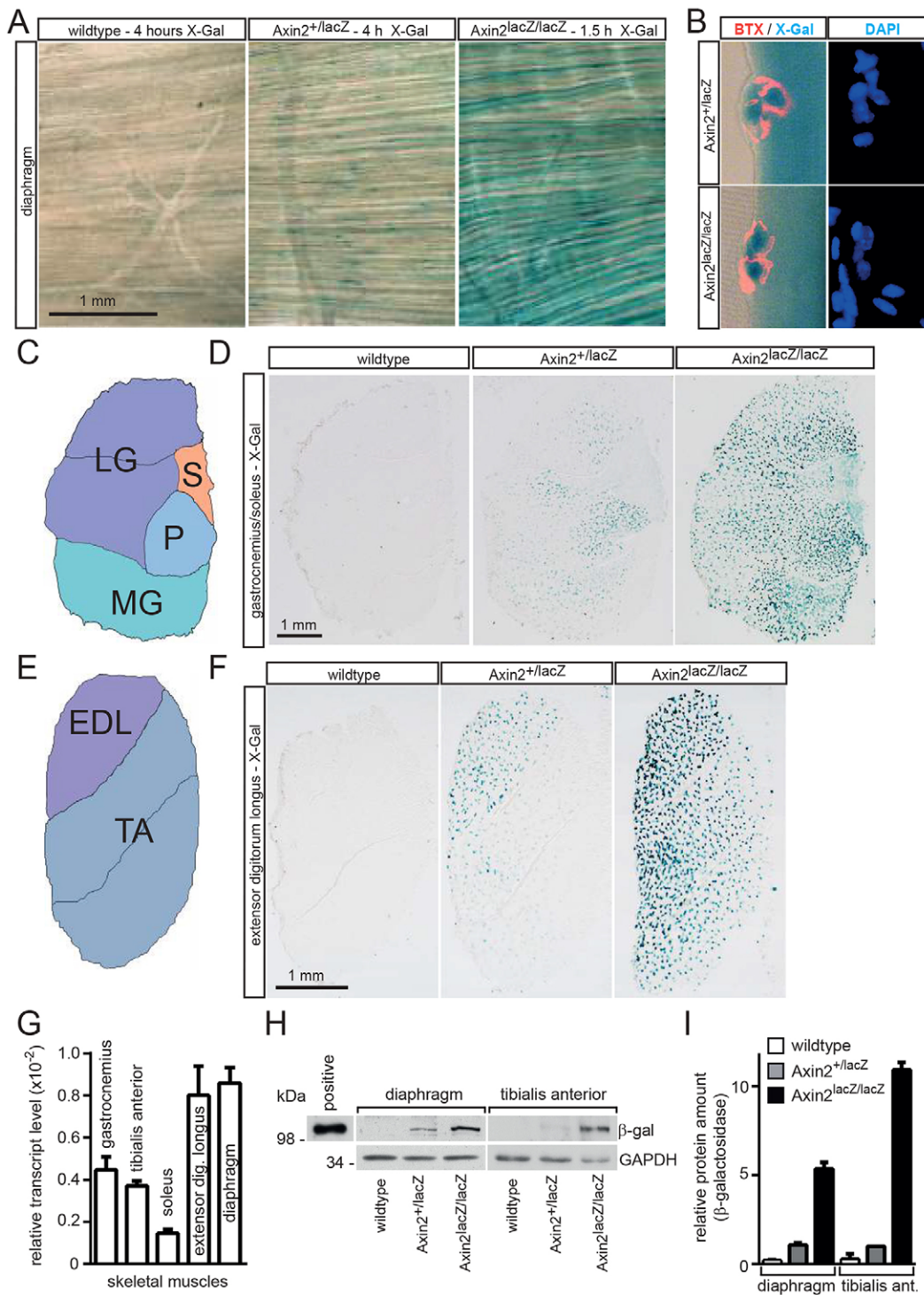


**Fig. 2. Activity of the *Axin2-lacZ* reporter in skeletal muscle cells.** (A) Diaphragms of wild-type mice and heterozygous and homozygous *Axin2-lacZ* reporter mice were subject to X-Gal staining for the times indicated. Owing to the strong blue staining the homozygous *Axin2-lacZ* diaphragm staining was stopped after 1.5 h, in contrast to 4 h for wild-type and heterozygous diaphragms. Note that only a fraction of muscle fibers are positively stained, even after extended staining duration and independent of whether heterozygous or homozygous *Axin2-lacZ* diaphragms were analyzed. (B) High-resolution images of whole-mount muscle fibers showing X-Gal-stained synaptic muscle nuclei underneath the pretzel-shaped neuromuscular junctions (stained with Rhodamine-conjugated  $\alpha$ -bungarotoxin, BTX). (C) Diagram indicating anatomical areas in the hindlimb gastrocnemius and soleus muscles. LG, gastrocnemius lateralis; P, plantaris; MG, gastrocnemius medialis; S, soleus. (D) X-Gal staining of frozen transverse sections of hindlimb gastrocnemius, plantaris and soleus muscles. (E) Diagram illustrating the hindlimb tibialis anterior (TA) and extensor digitorum longus (EDL) muscles. (F) Frozen transverse sections of hindlimb tibialis and extensor digitorum longus muscles stained with X-Gal. (G) Transcript levels of *Axin2* measured in different skeletal muscles by quantitative RT-PCR. In soleus muscle very little *Axin2* mRNA is detected. Error bars represent s.e.m.  $n=3$  wild-type mice. (H) Western blot of tissue lysates of  $\beta$ -gal-expressing muscles. There is a significant increase in  $\beta$ -gal protein in homozygous versus heterozygous *Axin2-lacZ* muscles. (I) Quantification of  $\beta$ -gal protein in the muscle lysates shown in H. Homozygous *Axin2-lacZ* muscles contain more than double the amount of  $\beta$ -gal protein predicted by gene dosage (5- to 10-fold greater than heterozygote). This significant increase results from the absence of *Axin2*, which is a negative effector of canonical Wnt signaling. Error bars represent s.d.  $n=3$  mice per genotype.

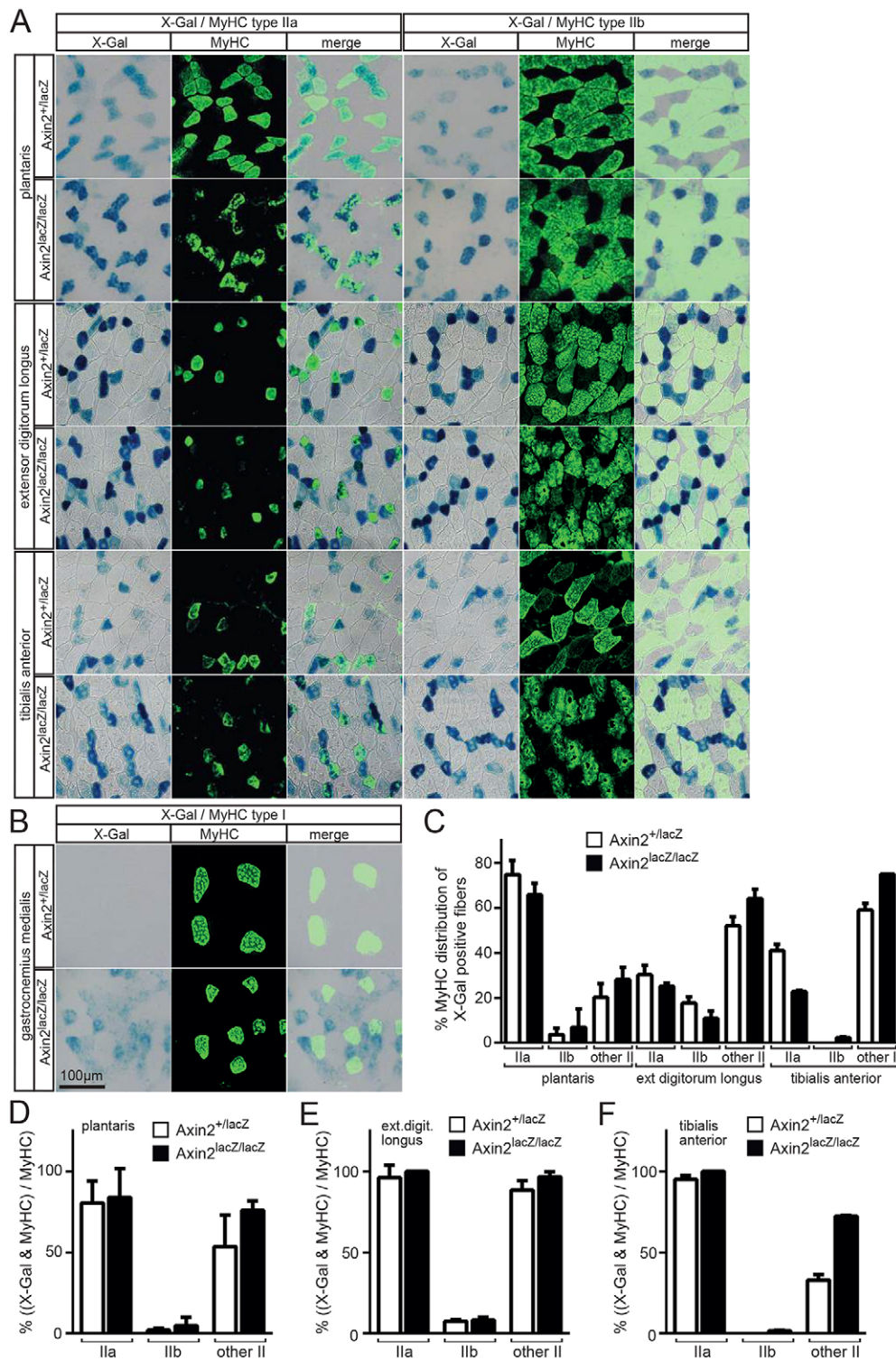


**Fig. 3. Identification of muscle fiber types expressing *Axin2* in wild-type and mutant skeletal muscles.** (A) The plantaris, extensor digitorum longus and tibialis anterior muscles of heterozygous and homozygous *Axin2-lacZ* reporter mice were dissected, transverse sectioned and stained. Representative immunofluorescence images for  $\beta$ -gal activity (X-Gal staining) and myosin heavy chain (MyHC) type IIa and IIb are shown. (B) The gastrocnemius medialis muscles of heterozygous and homozygous *Axin2-lacZ* reporter mice were transverse sectioned and stained for MyHC type I and for  $\beta$ -gal. Note that type I fibers are not  $\beta$ -gal positive. (C) Distribution of  $\beta$ -gal-positive muscle fibers belonging to types IIa, IIb or other type II in plantaris, extensor digitorum longus and tibialis anterior. (D-F) The proportion of each fiber type II subpopulation in the indicated muscles that stain positively for  $\beta$ -gal activity by X-Gal. Error bars represent s.d.  $n=3$  mice per genotype.

analyzed the gastrocnemius medialis, which contains a few type I fibers. However, the type I fibers in this muscle are not  $\beta$ -gal positive (Fig. 3B). Finally, for each muscle we asked what proportion of the total population of specific subtype II fibers are  $\beta$ -gal positive. In fact, regardless of whether *Axin2-lacZ* heterozygous or homozygous, almost all type IIa fibers were  $\beta$ -gal positive in plantaris, extensor digitorum and tibialis anterior (Fig. 3D-F). Moreover, in all three muscles type IIb fibers were rarely  $\beta$ -gal positive (Fig. 3D-F). The population of other type II

fibers that are  $\beta$ -gal positive is lower in plantaris and tibialis anterior than in extensor digitorum longus (Fig. 3D-F).

#### Muscle fibers that display active canonical Wnt/ $\beta$ -catenin signaling are of smaller diameter

To confirm that  $\beta$ -gal-positive fibers in heterozygous and homozygous *Axin2-lacZ* muscles indeed show active canonical Wnt signaling, transverse sections of hindlimb muscle were stained for  $\beta$ -gal,  $\beta$ -catenin, laminin and with DAPI (Fig. 4A). Most of the

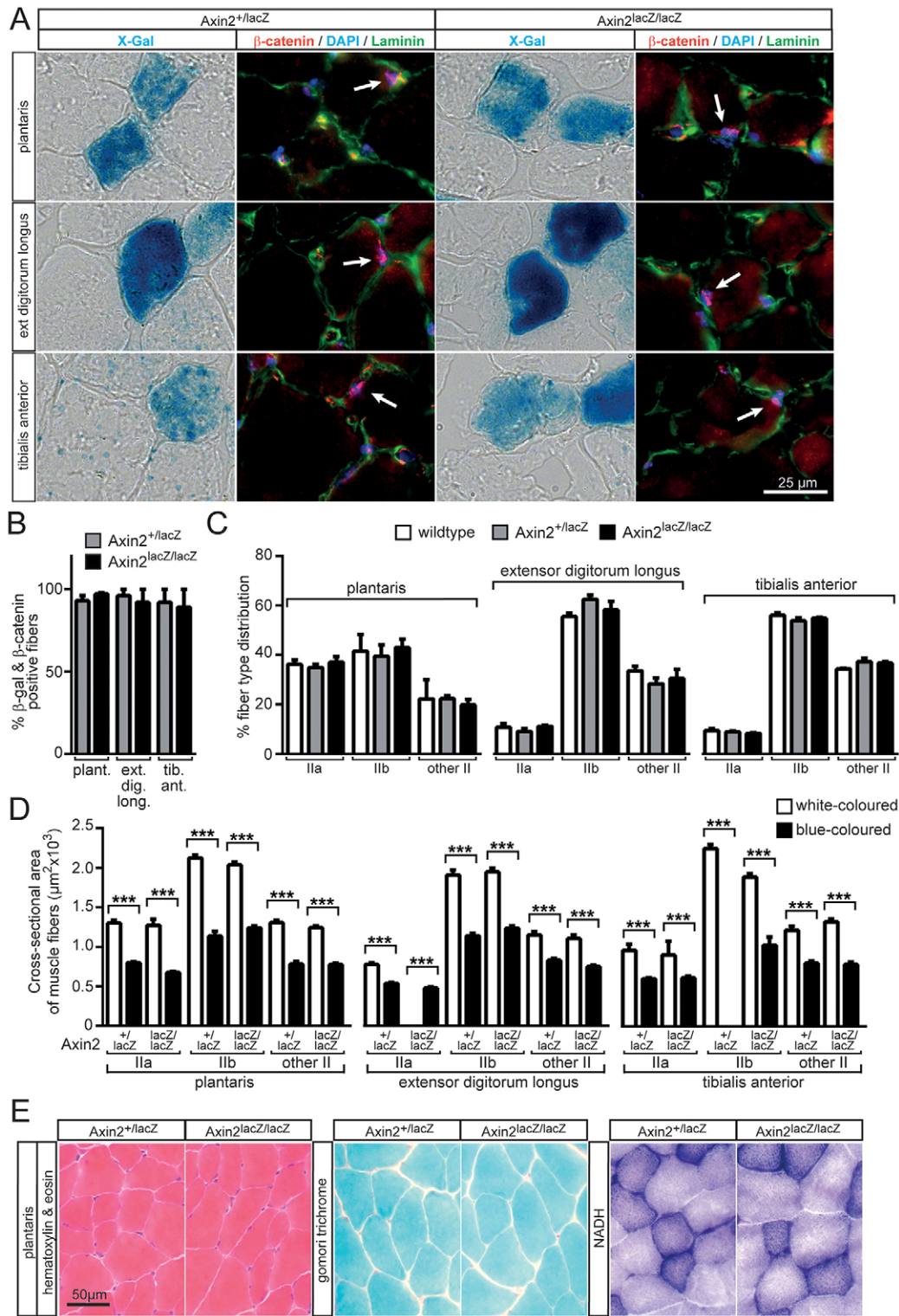


**Fig. 4. β-gal-positive Axin2-lacZ mutant skeletal muscle fibers contain nuclear β-catenin, have a lower cross-sectional area, but show no histological defects.** (A) Adjacent transverse sections of heterozygous and homozygous *Axin2-lacZ* plantaris, extensor digitorum longus and tibialis anterior muscles were either X-Gal stained or immunostained with a β-catenin-specific antibody. Most β-gal-positive fibers also show a nuclear β-catenin staining pattern (arrows). DAPI was used to stain nuclei and a laminin-specific antibody was used to label cell borders. (B) The percentage of fibers that are positive for both β-gal and nuclear β-catenin. (C) Muscle fiber type distribution in the three different skeletal muscles for wild-type and *Axin2-lacZ* mutants. No significant fiber type remodeling was observed among the genotypes. In B and C, error bars represent s.d.; *n*=3 mice per genotype. (D) Muscle fiber cross-sectional surface area (μm<sup>2</sup>) of type IIa, IIb, and most likely IIx (labeled as other type II) was measured for β-gal-negative and β-gal-positive fibers of the three muscles. Compared with β-gal-negative fibers of the same fiber type, all β-gal-positive fibers have a significantly smaller cross-sectional surface area. \*\*\**P*<0.001 (unpaired two-tailed *t*-test). Error bars represent s.e.m. *n*=3 mice per genotype, *n*>60 fibers per experiment. (E) Heterozygous and homozygous *Axin2-lacZ* plantaris muscles compared by H&E, Gomori trichrome and NADH staining. Representative images are shown.

$\beta$ -gal-positive muscle fibers within the plantaris, extensor digitorum longus and tibialis anterior muscles also showed expression of nuclear  $\beta$ -catenin (Fig. 4B). To exclude any muscle fiber type switch in the absence of Axin2, the distribution of all type II fibers was quantified for wild-type, heterozygous and homozygous *Axin2-lacZ* plantaris, extensor digitorum longus and tibialis anterior muscles. Importantly, no difference in fiber type distribution between the different genotypes was observed (Fig. 4C).

Next, we measured the cross-sectional areas of  $\beta$ -gal-positive fibers to investigate whether canonical Wnt signaling was related to changes in fiber size. Intriguingly, in heterozygous and homozygous *Axin2-lacZ* genotypes the  $\beta$ -gal-positive fibers of plantaris, extensor digitorum longus and tibialis anterior muscles were significantly smaller in cross-sectional area than  $\beta$ -gal-negative fibers, and this was true for all type II fiber types (Fig. 4D). Furthermore, no difference in cross-sectional area of type II fibers was detected between  $\beta$ -gal-positive heterozygous or homozygous *Axin2-lacZ* reporter muscles (Fig. 4D). Additional histological stainings were performed to exclude muscle impairments due to the absence of Axin2 in homozygous *Axin2-lacZ* muscle fibers. Indeed, no obvious changes in general morphology or oxidative metabolism were detected when employing Hematoxylin and Eosin (H&E), Gomori trichrome or NADH staining (Fig. 4E). Finally, we did not observe any signs of myopathy in the homozygous mice, as the number of fibers with centrally located nuclei or apoptotic cells was similar in the plantaris muscles of heterozygous and homozygous *Axin2-lacZ* reporter mice (data not shown).

#### Hippo pathway members YAP/Taz and Tead1 colocalize with canonical Wnt signaling in skeletal muscle fibers

Previously, a role for Taz in Wnt signaling was identified and subsequently confirmed by YAP/Taz incorporation into the  $\beta$ -catenin-containing destruction complex, which orchestrates the Wnt response (Azzolin et al., 2014, 2012). Moreover, the Hippo pathway effector YAP was demonstrated to be a crucial regulator of skeletal muscle fiber size (Watt et al., 2015). To further examine the potential correlation between canonical Wnt and YAP/Taz signaling, transverse sections of plantaris, extensor digitorum longus and tibialis anterior muscles were immunostained for Tead1 and YAP/Taz, and co-stained for laminin,  $\beta$ -gal and with DAPI (Fig. 5A,B). We found that the majority of  $\beta$ -gal-positive small-diameter fibers were also positive for Tead1 and YAP/Taz, regardless of whether they were from heterozygous or homozygous *Axin2-lacZ* mice (Fig. 5A–D), supporting the interplay between YAP/Taz and canonical Wnt signaling.

#### Wnt/ $\beta$ -catenin signaling is inactive in resting satellite cells but active in regenerating muscle fibers after injury

To further investigate Wnt/ $\beta$ -catenin signaling in skeletal muscle, we performed X-Gal staining in satellite cells. For this we used floating single-fiber cultures of extensor digitorum longus muscle from heterozygous *Axin2-lacZ* reporter mice. Interestingly, all  $\beta$ -gal-positive nuclei belonged to muscle fibers (Fig. 6). In fact, no satellite cells (marked by Pax7 expression) were  $\beta$ -gal positive, regardless of whether they were attached to  $\beta$ -gal-positive or  $\beta$ -gal-negative muscle fibers and regardless of whether they were quiescent or proliferating, as observed after 3 days of culture. Furthermore, no change in the number of quiescent satellite cells (Pax7-positive cells at day 0 of culture) was detected in  $\beta$ -gal-positive (mean  $5.80 \pm 1.16$ ) or  $\beta$ -gal-negative muscle fibers (mean  $5.47 \pm 0.44$ ), suggesting that Axin2 expression in the muscle fiber does not influence satellite cell numbers.

Next, we analyzed the expression of Axin2 during regeneration of skeletal muscle after injury. For this, we injected cardiotoxin (CTX) into the tibialis anterior muscle of adult wild-type, heterozygous and homozygous *Axin2-lacZ* mice. We observed  $\beta$ -gal expression by X-Gal staining in centrally located nuclei of newly formed myofibers in heterozygous and homozygous *Axin2-lacZ* mice (Fig. 7A). We further asked whether the time required for the formation of new fibers after CTX-induced injury differs in the absence of Axin2. The proportion of regenerating fibers expressing developmental MyHC after CTX injury was similar in wild-type, heterozygous and homozygous *Axin2-lacZ* muscles (Fig. 7B). Mononucleated muscle cells, regardless of whether they expressed Pax7 or MyoD (Myod1), were  $\beta$ -gal negative, further supporting the notion that satellite cells do not exhibit Wnt/ $\beta$ -catenin signaling (Fig. 7C,D).

#### Cross-talk between canonical Wnt/ $\beta$ -catenin and YAP/Taz/Tead1 signaling in muscle cells

To examine the influence of canonical Wnt/ $\beta$ -catenin signaling and YAP/Taz/Tead1-mediated gene transcription in muscle cells, the roles of Axin1, Axin2,  $\beta$ -catenin and Tead1 were studied in a series of knockdown experiments. First, axin-specific shRNAs were designed, evaluated and used for transfection of cultured primary myoblasts. The number of proliferating myoblasts was significantly lower in cells treated with shRNA against *Axin1* and both axins than in mock-transfected cells (Fig. 8A). The number of proliferating myoblast cells did not differ in cells transfected with shRNA against *Axin2* versus a mock control (Fig. 8A).

We then differentiated the cells and first evaluated the total number of myotubes per area after 2, 3 and 4 days. Interestingly, whereas myotube numbers were comparable to those of mock-transfected cells in the absence of Axin1, the number of myotubes was significantly reduced in the absence of Axin2, and regardless of whether shRNA against *Axin2* alone or together with shRNA against *Axin1* was used (Fig. 8B). Second, we tested whether YAP/Taz/TEAD signaling is stimulated during muscle cell differentiation. We transfected a GTIIC-luciferase reporter plasmid (a synthetic YAP/TAZ-responsive luciferase reporter; Fig. 8C) into cultured primary myoblasts. Interestingly, we detected a stimulation of YAP/Taz/TEAD signaling during muscle cell differentiation (Fig. 8C). Third, we asked whether an increase of YAP/Taz/TEAD signaling in myotubes (Fig. 8C) is accompanied by an increase in the expression of Tead1 target genes. Indeed, transcript levels of Tead1 target genes, such as *Ctgf*, *Ankrd1* and *Cyr61*, increased significantly during the differentiation of muscle cells (Fig. 8D). Fourth, we analyzed the specificity of canonical Wnt/ $\beta$ -catenin signaling activity in muscle cells during differentiation by knocking down either  $\beta$ -catenin or Tead1 and monitoring TOPflash activity (Fig. 8E). Knockdown of  $\beta$ -catenin, but not Tead1, significantly reduced TOPflash activity (Fig. 8E). Fifth, we asked how the GTIIC-luciferase reporter responds to the knockdown of either  $\beta$ -catenin or Tead1. Knockdown of Tead1 significantly reduced reporter activity, whereas knockdown of  $\beta$ -catenin stimulated the GTIIC-luciferase reporter (Fig. 8F). Sixth, we analyzed the influence of  $\beta$ -catenin or Tead1 knockdown on muscle cell differentiation. In the absence of either  $\beta$ -catenin or Tead1, there was a significant increase in myotube formation (Fig. 8G).

#### Canonical Wnts regulate the influence of $\beta$ -catenin/TCF/LEF and Tead1 on myoblast proliferation and differentiation

To understand whether canonical Wnts alter myogenic differentiation by regulating canonical Wnt and TEAD signaling, the response to dickkopf 1 (Dkk1) and stimulation by different Wnts was studied by TOPflash and GTIIC-luciferase reporter assays in

transiently transfected cultured differentiating primary myoblasts and myotubes. The specificity of intrinsic Wnt-dependent TOPflash stimulation during the differentiation of cultured muscle cells was

confirmed by inhibition of TOPflash stimulation in the presence of Dkk1, which specifically inhibits the canonical Wnt signaling pathway by the disruption of the Wnt-Fzd LRP complex (Krupnik

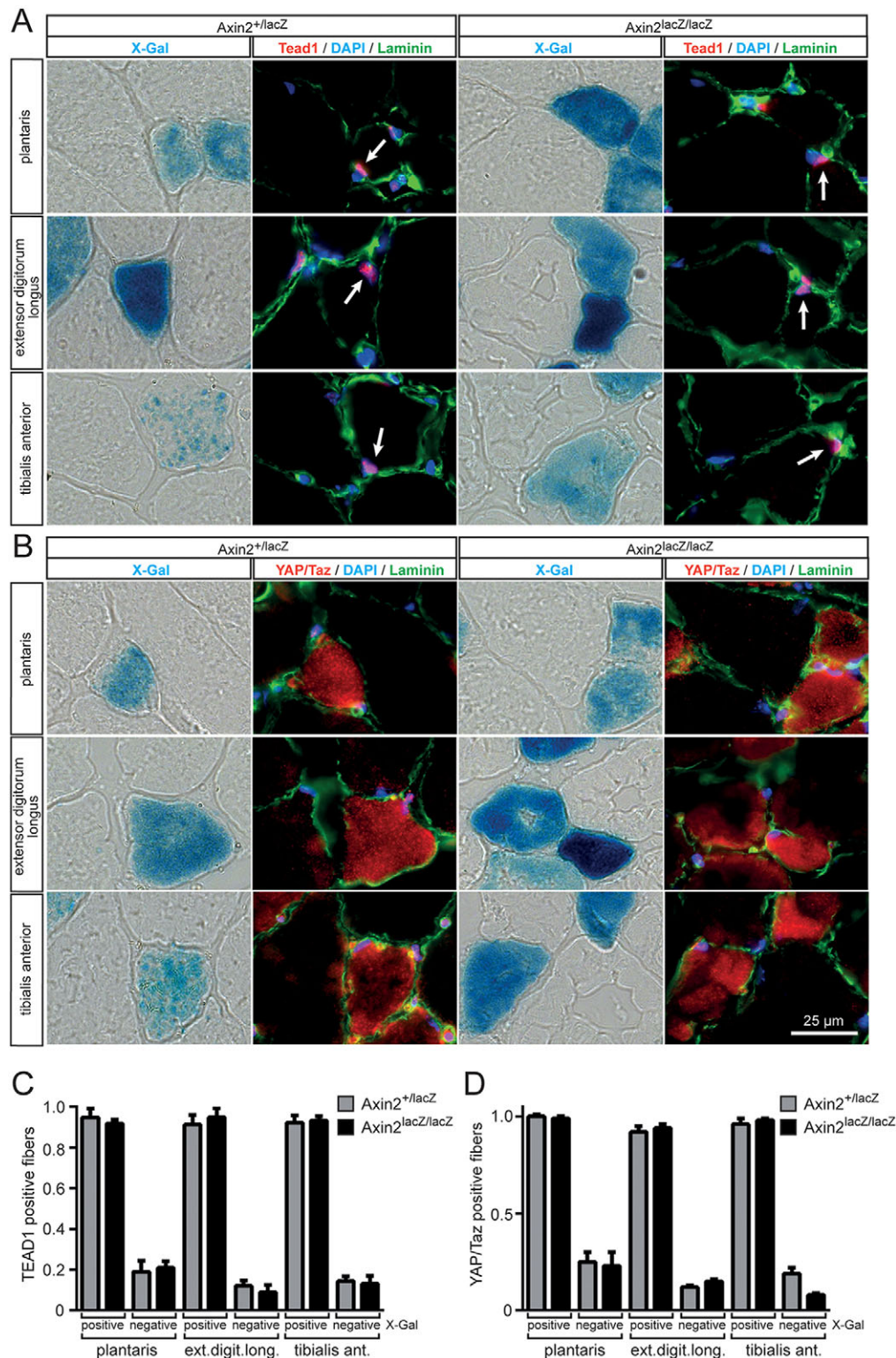


**Fig. 5.  $\beta$ -gal-positive *Axin2-lacZ* mutant muscle fibers are immunopositive for YAP/Taz and Tead1 antibodies.** (A,B) Adjacent transverse sections of heterozygous and homozygous *Axin2-lacZ* plantaris, extensor digitorum longus and tibialis anterior muscle were subject to X-Gal staining, or immunostained for Tead1 (A) or YAP/Taz (B), laminin and with DAPI. It is mainly  $\beta$ -gal-positive fibers that contain Tead1-positive nuclei (A, arrows). YAP/Taz also colocalize with X-Gal staining (B). (C,D) Quantification of Tead1-positive (C) or YAP/Taz-positive (D) fibers in relation to X-Gal staining and mouse genotype. Error bars represent s.d.  $n=3$  mice per genotype.



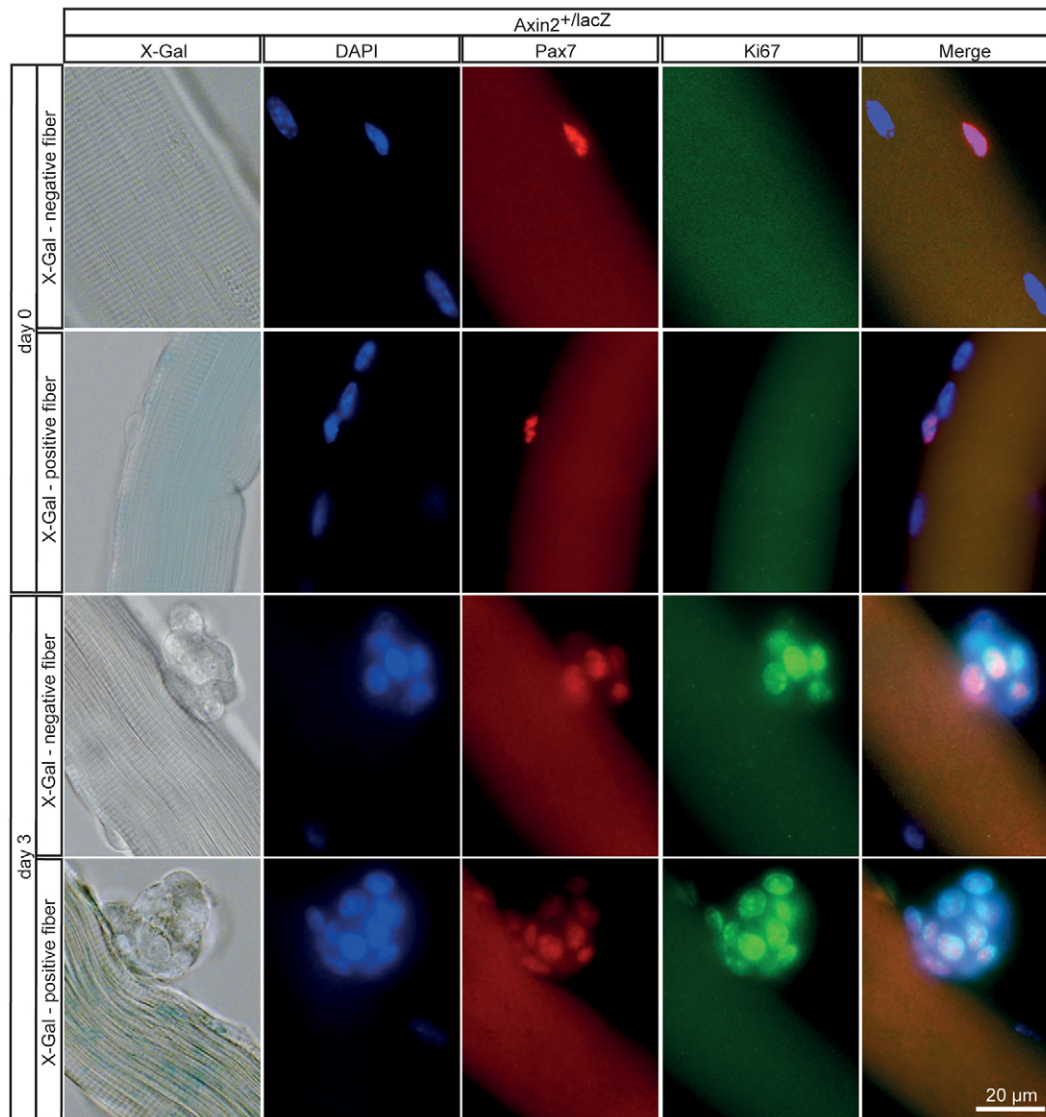


**Fig. 6. Axin2 expression pattern in muscle satellite cells.** Typical images of isolated single fibers of extensor digitorum longus muscles from heterozygous *Axin2-lacZ* mice. The fibers were either used immediately after isolation (day 0) or after 3 days of culture for staining with X-Gal, DAPI, Pax7 and Ki67 antibodies as indicated. Pax7-positive quiescent and proliferating muscle satellite cells were never  $\beta$ -gal positive, regardless of whether located on  $\beta$ -gal-negative or  $\beta$ -gal-positive muscle fibers.

et al., 1999) (Fig. 9A). Moreover, stimulation of TOPflash in differentiating myotubes was significantly accelerated by concomitant transfection of a plasmid encoding the canonical Wnt3a, but not if a plasmid encoding non-canonical Wnt7a was used (Fig. 9B). Next, we asked whether Wnts are able to stimulate the GTIIC-luciferase reporter as a means to monitor activation of YAP/Taz/TEAD signaling (Fig. 9C). Indeed, canonical Wnt3a induced GTIIC-luciferase activity during myotube differentiation. Importantly, this effect was inhibited by Dkk1, demonstrating the specificity of the signal (Fig. 9C).

Previously, it was shown that Axin2 is upregulated by Wnt signaling (Jho et al., 2002; Leung et al., 2002; Lustig et al., 2002), indicating that it is engaged in a negative-feedback loop controlling the cellular Wnt response. Indeed, knockdown of Axin2 was shown to increase  $\beta$ -catenin levels after Wnt stimulation (Bernkopf et al., 2015). To test whether the upregulation of Axin2 observed upon myotube formation is mediated by secreted canonical Wnt proteins we treated differentiating C2C12 cells with soluble Dkk1.

Cultivation of myotubes, after 3 days of differentiation, with Dkk1 for 24 h resulted in near-complete loss of Axin2 expression (Fig. 9D). This demonstrates that the canonical Wnt/ $\beta$ -catenin pathway is activated in differentiating myocytes by canonical Wnt ligands, and that this activation is responsible for the expression of Axin2.

We next analyzed whether Wnt3a would also alter myogenic differentiation. *Wnt3a* cDNA was delivered via retroviral infection of C2C12 cells, which were subsequently selected for stable integration of the viral cDNA. All investigations were performed with these polyclonal cell populations. Overexpression of Wnt3a induced an elongated cell morphology in myoblasts, as compared with control cells infected with empty vector (Fig. 9E, top panel). Activation of the canonical Wnt pathway was demonstrated by increased levels of cytosolic  $\beta$ -catenin using western blot analysis (data not shown). Importantly, when Wnt3a-overexpressing cells were cultured in differentiation medium, cells did not form multinucleated myotubes, in contrast to control cells (Fig. 9E, bottom panel). Impaired differentiation of C2C12 cells by incubation with Wnt3a-

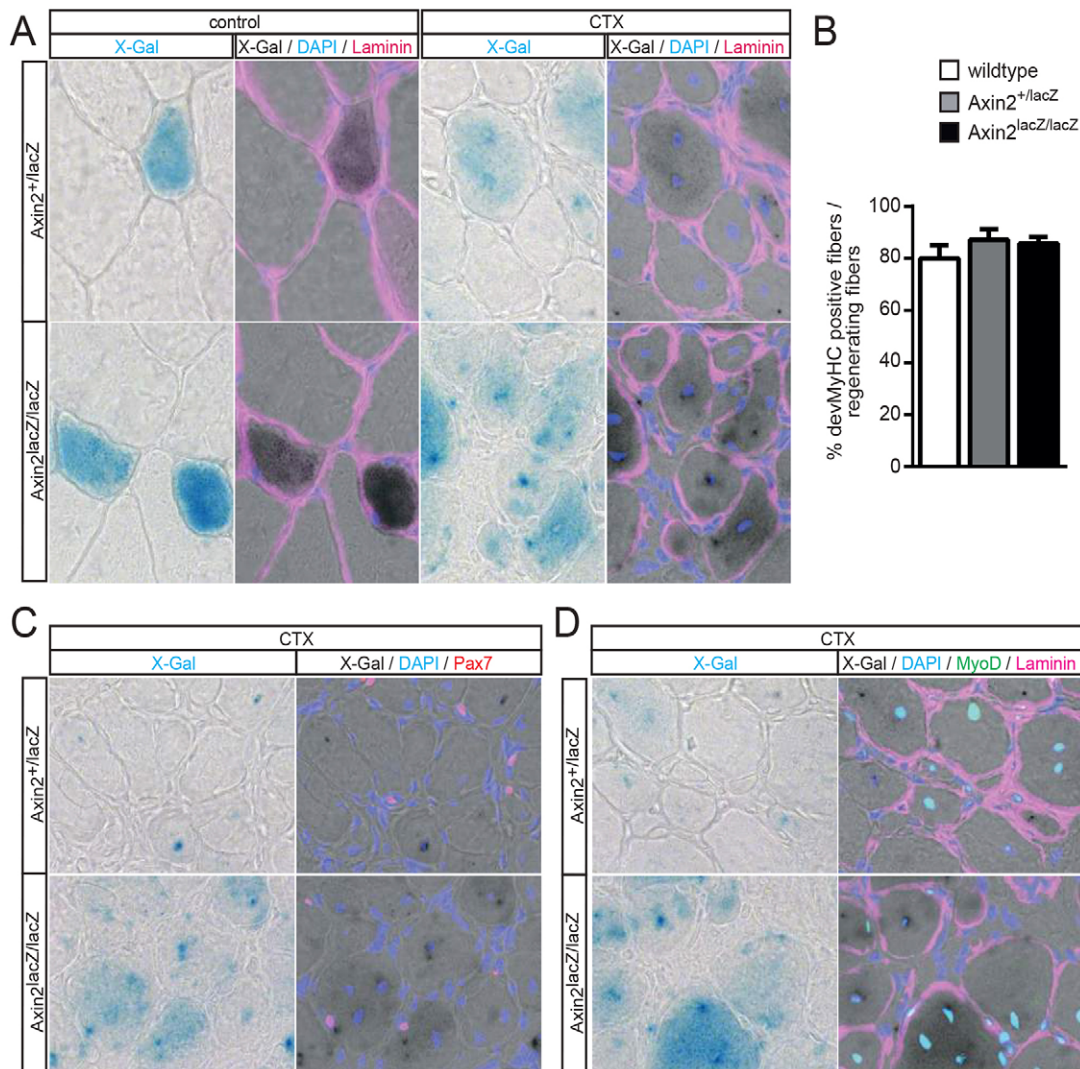


**Fig. 7. Axin2 is expressed in central nuclei after cardiotoxin-induced injury.** (A) Representative images of tibialis anterior muscle from heterozygous and homozygous *Axin2-lacZ* mice after cardiotoxin (CTX)-induced injury or under steady state conditions (control). Transverse sections were generated 10 days after treatment and stained for  $\beta$ -gal, laminin and with DAPI as indicated. Control muscles show X-Gal staining in muscle fibers, whereas CTX-treated muscles show additional X-Gal staining in central nuclei, most likely of regenerated fibers. (B) Quantification of developmental MyHC-positive fibers among the total regenerating fiber population. Error bars represent s.d.  $n=2$  wild type, 6 hetero- and 3 homozygous *Axin2-lacZ* mice. (C,D) Representative images show transverse sections of untreated and CTX-treated tibialis anterior muscle stained with X-Gal, DAPI, or for Pax7 or MyoD and laminin. Pax7-positive or MyoD-positive muscle satellite cells were never positive for  $\beta$ -gal.

conditioned medium was further confirmed by MyHC analysis (Fig. 9F,G). Lysates of C2C12 cells contained significant amounts of MyHC after 2 days of differentiation, but this increase did not occur in cells incubated with Wnt3a (Fig. 9F). Lack of MyHC expression and myotube formation was further confirmed by immunofluorescence staining of C2C12 cells (Fig. 9G).

The impairment of myotube formation by knockdown of Axin2 or treatment with canonical Wnts implies that overactivation of Wnt signaling is detrimental to myogenic differentiation. This is in line with several publications showing that activated  $\beta$ -catenin modulates myogenic differentiation (Gavard et al., 2004; Goichberg et al., 2001; Martin et al., 2002; Rudolf et al., 2016).

## DISCUSSION

This is, to our knowledge, the first report describing active canonical Wnt together with YAP/Taz/TEAD signaling in adult skeletal muscle fibers. Using *Axin2-lacZ* reporter mice, we identified active canonical

Wnt signaling in type II myofibers (Fig. 2) (Lustig et al., 2002). This mouse model is well established for tracing active canonical Wnt signaling since *Axin2* is a direct target of  $\beta$ -catenin-mediated gene expression (Barolo, 2006). In fact, heterozygous *Axin2-lacZ* mice, without any known signs of haploinsufficiency, express muscular  $\beta$ -gal in type II muscle fibers, suggesting that active canonical Wnt signaling is present physiologically in adult muscle fibers (Fig. 2). In homozygous *Axin2-lacZ* mice, not only is the doubled *lacZ* gene dosage responsible for elevated *Axin2-lacZ* reporter expression, but also the derepression of canonical Wnt signaling, since Axin2 itself is a negative regulator and target of canonical Wnt signaling and therefore participates in a negative-feedback loop. In fact, we detected a 5- to 10-fold increase in  $\beta$ -gal protein in muscles of homozygotes as compared with heterozygous *Axin2-lacZ* reporter mice (Fig. 2H,I). However, in *Axin2-lacZ* reporter mice only muscle fiber types IIa and IIx (shown for IIx indirectly) are positive for  $\beta$ -gal activity, suggesting that only these fibers display active canonical Wnt signaling (Fig. 3).

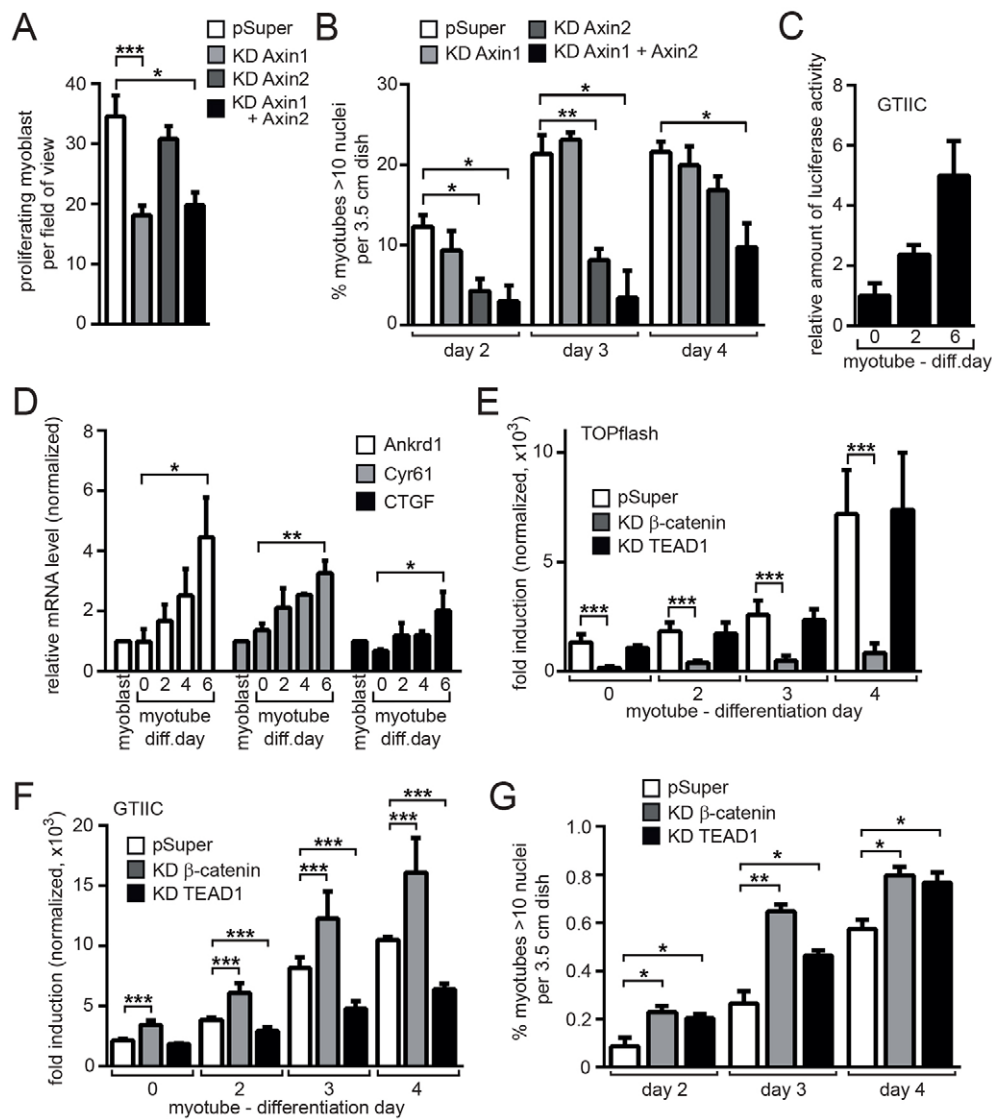


**Fig. 8. Characterization of the role of canonical Wnt and YAP/Taz/TEAD signaling in cultured muscle cells.** (A) Knockdown of Axin1 in primary muscle cell cultures under proliferating conditions significantly reduces the number of cells; this is independent of concomitant knockdown of Axin2. (B) The same cells as depicted in A were continuously monitored to assess how well they are able to fuse to multinucleated myotubes. Knockdown of Axin2, independent of concomitant knockdown of Axin1, significantly delayed myotube formation (day 2 and 3). By day 4, myotube formation had caught up in cells in which Axin2 was knocked down. (C) The GTIIC-luciferase reporter reflects TEAD-dependent gene expression activity. The reporter was transfected into cultured primary muscle cells, which were then differentiated for the indicated number of days, before lysate preparation and luciferase activity measurement. Note that intrinsic normalized reporter activity increased gradually upon differentiation. (D) Changes in transcript levels of endogenous Tead1 target genes upon differentiation of muscle cells. *Ankrd1*, *Cyr61* and *CtGF* transcript levels significantly increased from day 0 to 6 in C2C12 cells. (E) Cultured primary muscle cells were transfected with TOPflash reporter together with either β-catenin or Tead1 knockdown plasmids, and were monitored for luciferase activity during differentiation. Knockdown of β-catenin, but not Tead1, inhibits the increase in endogenous canonical Wnt signaling activity. (F) A similar experiment to that in E but with GTIIC-luciferase reporter. Knockdown of Tead1 significantly stalled GTIIC reporter activity during differentiation, whereas knockdown of β-catenin significantly increased reporter activity. (G) After knockdown of either β-catenin or Tead1, the number of primary cultured myotubes was quantified at different time points of differentiation, as indicated. Note that muscle cell differentiation is accelerated if either β-catenin or Tead1 is knocked down. \* $P < 0.05$ , \*\* $P < 0.01$ , \*\*\* $P < 0.001$  (unpaired two-tailed *t*-test). Error bars represent s.e.m. (A,B,G) or s.d. (C-F).  $n = 5$  sets of cells, each as duplicate, except in D where  $n = 3$  sets of cells and  $n = 3$  qPCR runs for each set of cells.

Interestingly, soleus muscle does not express any significant amounts of β-gal in heterozygous or homozygous *Axin2-lacZ* reporter mice, suggesting that Wnt signaling is inactive in this particular muscle (Fig. 2D). Furthermore, the specificity of muscle cell-specific canonical Wnt signaling was confirmed when the endogenous Wnt-dependent stimulation of TOPflash reporter in cultured primary muscle cells was inhibited by *Dkk1*, an extracellular inhibitor of canonical Wnt signaling (Fig. 9A).

Previously, the only report concerning canonical Wnt signaling in adult skeletal muscle fibers employed *TCF-lacZ* transgenic

reporter mice, using a promoter with artificial multimerized TCF binding sites to drive transcription of the *lacZ* reporter gene (Kuroda et al., 2013). It was shown that canonical Wnt signaling is strongly activated during fetal myogenesis and weakly activated in slow myofibers of adult muscles (Kuroda et al., 2013). Intriguingly, in contrast to those data, we find that canonical Wnt signaling is absent from slow type I muscle fibers (Fig. 2C, Fig. 3B). These contradictory data might be explained by the fact that the *Axin2-lacZ* reporter mouse better represents the physiological condition, since the *lacZ* gene is driven by the endogenous *Axin2* promoter.

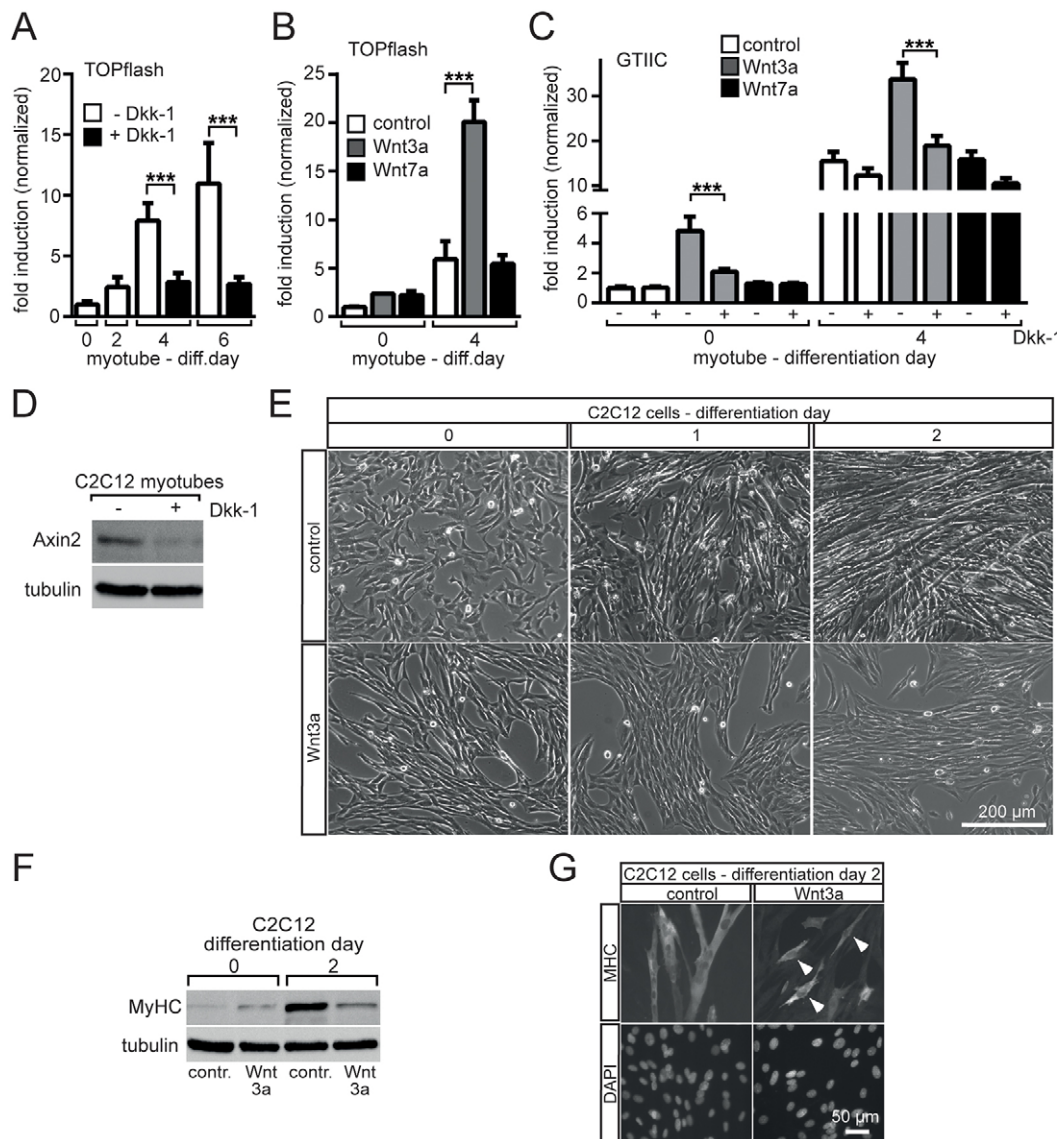


**Fig. 9. Canonical Wnts regulate Wnt/ $\beta$ -catenin and YAP/Taz/TEAD signaling in differentiating muscle cells.** (A) Canonical Wnt-dependent endogenous activation of TOPflash reporter during differentiation was verified by co-transfection of Dkk1, an extracellular inhibitor of canonical Wnt signaling, into cultured primary muscle cells. In the presence of Dkk1, endogenous upregulation of the TOPflash activity was significantly blocked. (B) Cultured primary muscle cells were transfected with TOPflash and canonical Wnt3a or non-canonical Wnt7a expression plasmids. Luciferase activity significantly increased during differentiation upon Wnt3a transfection in comparison to the control. (C) Influences of canonical and non-canonical Wnts on GTIIC-luciferase reporter activity were investigated with or without Dkk1 using cultured primary muscle cells. Wnt and Dkk1 expression plasmids were transfected as indicated. Luciferase activity was measured at days 0 and 4 of myotube differentiation. The Wnt3a-mediated increase of GTIIC reporter activity is abolished by Dkk1 at days 0 and 4.  $***P < 0.001$  (unpaired two-tailed *t*-test). In A–C, error bars represent s.d.;  $n = 5$  sets of cells, each as duplicate. (D) Western blot analysis showing that Dkk1 suppresses the expression of Axin2 in C2C12 myotubes. (E) Culture of C2C12 cells infected with empty vector (control) or with Wnt3a cDNA in differentiation medium for 2 days. Wnt3a-expressing C2C12 cells did not form multinucleated myotubes. (F) Expression of Wnt3a prevents upregulation of MyHC. C2C12/pLNCX2 (control) and C2C12/Wnt3a cells were cultured in differentiation medium for 2 days and lysates subjected to western blot analysis. On day 0, MyHC was slightly increased in C2C12/Wnt3a cells compared with control cells, but was not upregulated during differentiation. (G) MyHC-expressing C2C12/Wnt3a cells remain mononucleated (arrowheads).

Importantly, the absence of Axin2 in adult homozygous *Axin2-lacZ* muscles does not result in any obvious muscle phenotype. Grip strength appeared to be marginally affected in young homozygous *Axin2-lacZ* mice (data not shown), but this remains to be investigated further in aged mice, where typically a muscle weakness phenotype is more prominent. Still, neither fiber type switches nor any histological or metabolic impairments were detected in mutant muscles (Fig. 4C,E). Therefore, in adult muscle fibers Axin2 appears to reflect the localization of active canonical Wnt signaling but without itself being of any

obvious importance for skeletal muscle under steady-state conditions.

Although general muscle biology is not affected by the absence of Axin2, muscle fibers with active Wnt signaling differ morphologically from neighboring fibers lacking canonical Wnt signaling. All muscle fibers that exhibited  $\beta$ -gal activity, regardless of whether they were from heterozygous or homozygous *Axin2-lacZ* reporter mice, had a significantly smaller cross-sectional area (Fig. 4D). As such, just by measuring the cross-sectional area it is, in principle, possible to identify muscle fibers active in canonical Wnt

signaling. Previously, a change of fiber diameter in regenerated fibers in the absence of  $\beta$ -catenin and APC was reported (Jones et al., 2015; Murphy et al., 2014; Parisi et al., 2015). As a first step towards understanding why canonical Wnt signaling is active in those muscle fibers, we speculated that the Hippo pathway might be involved, since it has been demonstrated that the Hippo pathway effector YAP is also a crucial regulator of skeletal muscle fiber size (Watt et al., 2015). Moreover, it has been shown that YAP/Taz are part of the  $\beta$ -catenin destruction complex and are involved in orchestrating the Wnt response (Azzolin et al., 2014, 2012). Thus far, it had not been investigated whether YAP regulates skeletal muscle fiber size in a fiber-type dependent manner (Watt et al., 2015). Another player might be Tead1, since a potential role for Tead1 signaling in muscle is promotion of a generally slower skeletal muscle contractile phenotype (Tsika et al., 2008). We detected YAP/Taz and Tead1 in the same fiber types in which canonical Wnt signaling was active (Fig. 5A–D). Moreover, the expression of the Tead1 target genes *Ctgf*, *Cyr61* and *Ankrd1* increased together with the increase in Axin2 expression in muscle cells (Fig. 1A–D, Fig. 8D). Altogether, these findings indicate that canonical Wnt signaling might act together with YAP/Taz/TEAD1-mediated signaling in the regulation of skeletal muscle fiber size. Interestingly, intrinsic gradual GTIIC-luciferase reporter activation, resembling the Axin2 expression profile and TOPflash activity, was detected during the differentiation of cultured primary muscle cells (Fig. 1, Fig. 8C). Knockdown of Tead1 did not influence TOPflash activity, suggesting that there is no feedback loop from Tead1 to canonical Wnt signaling (Fig. 8E). However, and in agreement with previously published data obtained in HEK293 cells showing that  $\beta$ -catenin stimulates Taz degradation (Azzolin et al., 2012), our data showed that knockdown of  $\beta$ -catenin increased GTIIC-luciferase activity. Furthermore, we show that the GTIIC-luciferase reporter responds to exogenous canonical Wnt stimulation (Fig. 9C), but is also sensitive to Dkk1, demonstrating the cross-talk between both pathways in skeletal muscle.

Interestingly, we also found that Axin2 is expressed in regenerating myofibers but not in quiescent or activated satellite cells (Figs 6, 7). Our experiments further show that endogenous Axin2 expression is absent in myoblasts (Fig. 1A,B,D), which is in accordance with recent data demonstrating that only very low levels of active  $\beta$ -catenin protein are found in undifferentiated muscle progenitors (Rudolf et al., 2016). We therefore speculate that canonical Wnt signaling is an important player in the differentiation process (from myoblasts to myotubes) but is not required for satellite cell maintenance. This fits well with previous reports describing Wnt/ $\beta$ -catenin activity as regulating satellite cell myogenic potential (Bernardi et al., 2011; Brack et al., 2008; Jones et al., 2015). However, Wnt-dependent TGF $\beta$ 2 signaling was reported to be important for the commitment of satellite cells to a non-myogenic lineage, with a shift towards a more fibrotic phenotype that is associated with increased TGF $\beta$  signaling in regenerating or diseased muscle (Biressi et al., 2014; Brack et al., 2007). Data obtained in our laboratory do not indicate any change in *Tgfb2* transcript level in Axin2-deficient muscles (data not shown).

Since Axin2 autoregulates its own expression by a negative-feedback loop, we suggest that the temporal activity and level of canonical Wnt signaling are controlled via Axin2. This tight regulation would halt activation of canonical Wnt signaling in the presence of Axin2, thereby avoiding transdifferentiation. To gain further insight into cell biological aspects of canonical Wnt signaling, changes in Axin expression were monitored in C2C12 and primary muscle cells (Figs 1 and 8). Previously, it was reported that Axin2 expression

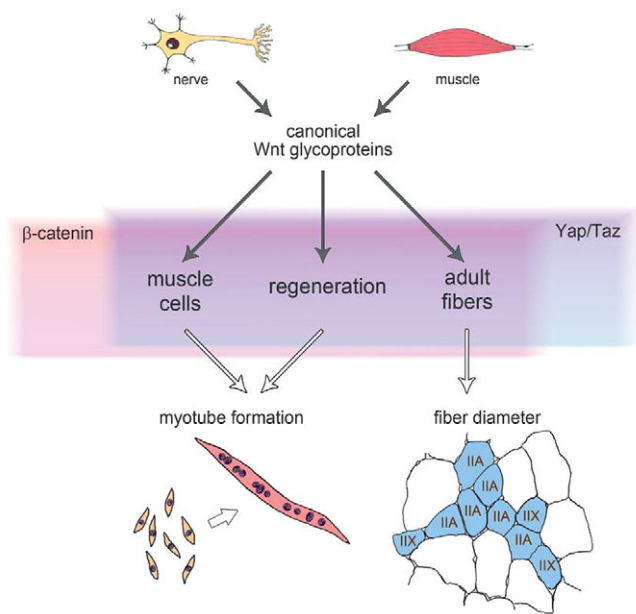


**Fig. 10. Model of how YAP/Taz/TEAD1 and  $\beta$ -catenin-dependent canonical Wnt signaling act on muscle cells to influence myotube formation and fiber type diameter.** Axin2/ $\beta$ -catenin and YAP/Taz/TEAD1 appear to act together (as indicated by the two colored shaded boxes) on muscle cells at various stages (myoblast, regeneration, adult fibers) to ensure proper differentiation to myotubes and the correct fiber diameter. For details see the Discussion.

increases during muscle cell differentiation *in vitro* (Bernardi et al., 2011; Figeac and Zammit, 2015). Here, we confirmed these data in primary muscle cell cultures and additionally demonstrated that Axin1 is constitutively expressed in myoblasts and myotubes (Fig. 1A–D). Knockdown experiments showed that Axin1 is required for the proliferation of myoblasts (Fig. 8A), whereas Axin2 is necessary for myotube formation (Fig. 8B). In the absence of Axin2, myotube formation was inhibited but not fully blocked, suggesting delayed differentiation upon strong activation of Wnt/ $\beta$ -catenin signaling. Similar results were obtained by addition of canonical Wnt3a to differentiating muscle cell cultures (Fig. 9E–G), further supporting the notion of delayed differentiation upon strong activation of Wnt/ $\beta$ -catenin signaling. Recent studies employing genetic non-degradable  $\beta$ -catenin mutants in satellite cell progeny reported controversial results concerning the muscle regeneration phenotype in loss- versus gain-of-function mutants, but both underline the necessity for strict regulation of  $\beta$ -catenin signaling activity during muscle regeneration (Murphy et al., 2014; Rudolf et al., 2016).

We present a model describing the interplay between canonical Wnt signaling and YAP/Taz/TEAD signaling in myofibers, and hypothesize that the Wnt glycoproteins might be supplied by the muscle cells themselves, providing them in an autocrine/paracrine fashion, and/or by the motor nerve endings (Fig. 10). During differentiation or regeneration, Axin2-mediated canonical Wnt signaling might be involved in myotube formation, whereas in adult muscle fibers Axin2-mediated canonical Wnt signaling and YAP/Taz/TEAD1-mediated signaling might ensure proper fiber size diameter in a subset of skeletal muscle fibers (Fig. 10).

## MATERIALS AND METHODS

### Constructs, knockdown and PCR

Silencing of *Axin1*, *Axin2*,  $\beta$ -catenin and *Tead1* was achieved using plasmid-derived shRNAs (see supplementary Materials and Methods). For the generation of *in situ* riboprobes, *Axin1* and *Axin2* fragments were PCR

amplified using the primers described in Table S1 and subcloned into pGEM-T Easy (Promega) (for details, see the supplementary Materials and Methods). Recombinant Dkk1 was produced essentially as described previously (Krupnik et al., 1999) (see supplementary Materials and Methods). pHAN-puro, pHAN-Wnt3a and pHAN-Wnt7a vectors were kindly gifted by Michael A. Rudnicki (Ottawa Hospital Research Institute, Canada). Total RNA was extracted from mouse tissues with TRIzol reagent (Life Technologies) (Cheusova et al., 2006). After reverse transcription, cDNAs were used with mouse-specific primers (Table S1) for quantitative PCR reactions using the ABsolute QPCR SYBR Green Capillary Mix (Fisher Scientific), glass capillaries and LightCycler (Roche Diagnostics) according to the manufacturers' instructions. Data analysis was performed as described (Cheusova et al., 2006).

### Tissue culture, culturing of primary muscle cells and transfection

Primary skeletal muscle cells were prepared from muscles of adult BL6 wild-type mice using the MACS Satellite Cell Isolation Kit (Miltenyi Biotec) according to the manufacturer's instructions. C2C12 and primary skeletal myoblasts were transiently transfected by nucleofection according to the manufacturer's instructions (Nucleofector, Lonza). Single myofibers were isolated from the extensor digitorum longus muscle by collagenase digestion and cultured as described elsewhere (von Maltzahn et al., 2013). Culture conditions and transfection protocols are provided in the supplementary Materials and Methods.

### In situ hybridization

*In situ* hybridization for *Axin1* and *Axin2* was performed as previously described (Schubert et al., 2008). A detailed protocol is provided in the supplementary Materials and Methods.

### Luciferase assays

TOPflash or GTIIC-luciferase reporter assays were performed using primary skeletal muscle cells or C2C12 myoblasts transiently transfected with luciferase reporter and other expression plasmids (hDkk1-Flag, pHAN-puro, pHAN-Wnt3a, pHAN-Wnt7a). After transfection, myoblasts were differentiated to myotubes, harvested at the indicated time points, and cell extracts prepared for luciferase assays. Where indicated, cells were exposed to control- or Dkk1-conditioned medium for 24 h before harvesting. Each sample was transfected in duplicate, and each experiment was repeated at least three times.

### SDS-PAGE and western blot

Equal amounts of extracted proteins were solubilized in Laemmli buffer, boiled, separated by SDS-PAGE and blotted to nitrocellulose membrane (Protran BA85, Whatman) or Immobilon membranes (Amersham). Membranes were blocked and incubated with primary antibodies at 4°C overnight. Corresponding secondary antibodies conjugated with horseradish peroxidase were used to detect primary antibodies. Protein bands were detected by chemiluminescence reaction and exposed on a LAS-3000 luminescence image analyzer (Fujifilm). Western blot results were quantified by densitometric analysis using ImageJ (<http://rsb.info.nih.gov/ij/>). For further details, including antibodies used, see the supplementary Materials and Methods.

### Mice

Mouse experiments were performed in accordance with animal welfare laws and approved by the responsible local committees (animal protection officer, Sachgebiet Tierschutzangelegenheiten, FAU Erlangen-Nürnberg, AZ: 1/39/EE006 and TS-07/11) and government bodies (Regierung von Unterfranken). Mice were housed in cages that were maintained in a room with temperature 22±1°C and relative humidity 50–60% on a 12-h light/dark cycle. Water and food were provided *ad libitum*. Mouse mating and genotyping were performed as previously described (Yu et al., 2005).

### CTX treatment

For muscle injury experiments mice were anesthetized and 50 µl cardiotoxin (Sigma; 10 µM in 0.9% NaCl) directly injected into the tibialis anterior

muscle. Mice were sacrificed 10 days after injury and muscles frozen in liquid nitrogen.

### Histochemical staining, immunohistochemistry and TUNEL assay

Detailed protocols for histochemical stainings, including X-Gal, H&E, Gomori trichrome and NADH, and for the TUNEL assay for apoptotic cells are provided in the supplementary Materials and Methods.

### Immunofluorescence staining, fluorescence microscopy, morphometry

For immunofluorescence analysis, transverse sections of muscle were permeabilized for 5–10 min in 0.1% Triton X-100 in PBS, blocked in 10% (v/v) FCS, 1% (v/v) BSA in PBS or M.O.M. blocking reagent (Mouse Ig Blocking Reagent, Vector Laboratories) for 1 h at room temperature. For analysis of satellite cells, single isolated muscle fibers were blocked in 5% (v/v) horse serum in PBS. Incubation with primary antibodies was performed overnight at 4°C. Fluorophore-coupled secondary antibodies were used for detection of primary antibodies and nuclei were counterstained with DAPI. Information on antibodies is provided in the supplementary Materials and Methods.

Effects on proliferation and primary myotube formation after knocking down axins were quantified using a Leica DM IRB microscope. For assessment of proliferation, myoblasts were fixed 48 h after transfection. Total myoblast numbers per 3.5 cm plate were counted that were positive for the co-transfected GFP expression. For myogenic differentiation analysis, GFP-positive myotubes containing more than ten myonuclei were counted and related to the GFP-positive total myotube number.

### Acknowledgements

pHAN-puro, pHAN-Wnt3a and pHAN-Wnt7a vectors were kindly gifted by Michael A. Rudnicki.

### Competing interests

The authors declare no competing or financial interests.

### Author contributions

Conceptualization: S.H., J.v.M., J.B.; Methodology: D.H., N.E., M.R., L.M.Z., B.K.; Investigation: D.H., N.E., M.R., L.M.Z., B.K., D.B.; Resources: D.B.; Writing – original draft preparation: S.H.; Writing – review and editing: S.H., J.v.M., J.B., D.H.; Supervision: S.H., J.v.M., J.B.; Project administration: S.H.; Funding acquisition: S.H., J.v.M., J.B.

### Funding

This work was supported by a grant from the German Research Foundation (Deutsche Forschungsgemeinschaft) [MA-3975/2-1] to J.v.M.; the Emerging Fields Initiative (EFI) of Friedrich-Alexander-Universität Erlangen-Nürnberg to J.B.; and the Interdisciplinary Center for Clinical Research Erlangen, at Universitätsklinikum Erlangen-Nürnberg project E17 to S.H.

### Supplementary information

Supplementary information available online at <http://dev.biologists.org/lookup/doi/10.1242/dev.139907.supplemental>

### References

- Agbulut, O., Noirez, P., Beaumont, F. and Butler-Browne, G. (2003). Myosin heavy chain isoforms in postnatal muscle development of mice. *Biol. Cell* **95**, 399–406.
- Armstrong, D. D. and Esser, K. A. (2005). Wnt/beta-catenin signaling activates growth-control genes during overload-induced skeletal muscle hypertrophy. *Am. J. Physiol. Cell Physiol.* **289**, C853–C859.
- Armstrong, D. D., Wong, V. L. and Esser, K. A. (2006). Expression of beta-catenin is necessary for physiological growth of adult skeletal muscle. *Am. J. Physiol. Cell Physiol.* **291**, C185–C188.
- Azzolin, L., Zanconato, F., Bresolin, S., Forcato, M., Basso, G., Bicciato, S., Cordenonsi, M. and Piccolo, S. (2012). Role of TAZ as mediator of Wnt signaling. *Cell* **151**, 1443–1456.
- Azzolin, L., Panciera, T., Soligo, S., Enzo, E., Bicciato, S., Dupont, S., Bresolin, S., Frasson, C., Basso, G., Guzzardo, V. et al. (2014). YAP/TAZ incorporation in the beta-catenin destruction complex orchestrates the Wnt response. *Cell* **158**, 157–170.
- Barolo, S. (2006). Transgenic Wnt/TCF pathway reporters: all you need is Lef? *Oncogene* **25**, 7505–7511.

- Behrens, J., Jerchow, B. A., Wurtele, M., Grimm, J., Asbrand, C., Wirtz, R., Kuhl, M., Wedlich, D. and Birchmeier, W. (1998). Functional interaction of an axin homolog, conductin, with beta-catenin, APC, and GSK3beta. *Science* **280**, 596-599.
- Bentzinger, C. F., von Maltzahn, J., Dumont, N. A., Stark, D. A., Wang, Y. X., Nhan, K., Frenette, J., Cornelison, D. D. and Rudnicki, M. A. (2014). Wnt7a stimulates myogenic stem cell motility and engraftment resulting in improved muscle strength. *J. Cell Biol.* **205**, 97-111.
- Bernardi, H., Gay, S., Fedon, Y., Vernus, B., Bonniou, A. and Bacou, F. (2011). Wnt4 activates the canonical beta-catenin pathway and regulates negatively myostatin: functional implication in myogenesis. *Am. J. Physiol. Cell Physiol.* **300**, C1122-C1138.
- Bernkopf, D. B., Hadjihannas, M. V. and Behrens, J. (2015). Negative-feedback regulation of the Wnt pathway by conductin/axin2 involves insensitivity to upstream signalling. *J. Cell Sci.* **128**, 33-39.
- Bhanot, P., Brink, M., Samos, C. H., Hsieh, J.-C., Wang, Y., Macke, J. P., Andrew, D., Nathans, J. and Nusse, R. (1996). A new member of the frizzled family from *Drosophila* functions as a Wntless receptor. *Nature* **382**, 225-230.
- Biressi, S., Miyabara, E. H., Gopinath, S. D., Carlig, P. M. and Rando, T. A. (2014). A Wnt-TGFbeta2 axis induces a fibrogenic program in muscle stem cells from dystrophic mice. *Sci. Transl. Med.* **6**, 267ra176.
- Blau, H. M., Chiu, C.-P. and Webster, C. (1983). Cytoplasmic activation of human nuclear genes in stable heterocaryons. *Cell* **32**, 1171-1180.
- Brack, A. S., Conboy, M. J., Roy, S., Lee, M., Kuo, C. J., Keller, C. and Rando, T. A. (2007). Increased Wnt signaling during aging alters muscle stem cell fate and increases fibrosis. *Science* **317**, 807-810.
- Brack, A. S., Conboy, I. M., Conboy, M. J., Shen, J. and Rando, T. A. (2008). A temporal switch from notch to Wnt signaling in muscle stem cells is necessary for normal adult myogenesis. *Cell Stem Cell* **2**, 50-59.
- Cadigan, K. M. and Nusse, R. (1997). Wnt signaling: a common theme in animal development. *Genes Dev.* **11**, 3286-3305.
- Cheusova, T., Khan, M. A., Schubert, S. W., Gavin, A. C., Buchou, T., Jacob, G., Sticht, H., Allende, J., Boldyreff, B., Brenner, H. R. et al. (2006). Casein kinase 2-dependent serine phosphorylation of MuSK regulates acetylcholine receptor aggregation at the neuromuscular junction. *Genes Dev.* **20**, 1800-1816.
- Clevers, H. (2006). Wnt/beta-catenin signaling in development and disease. *Cell* **127**, 469-480.
- Eastman, Q. and Grosschedl, R. (1999). Regulation of LEF-1/TCF transcription factors by Wnt and other signals. *Curr. Opin. Cell Biol.* **11**, 233-240.
- Figec, N. and Zammit, P. S. (2015). Coordinated action of Axin1 and Axin2 suppresses beta-catenin to regulate muscle stem cell function. *Cell Signal.* **27**, 1652-1665.
- Gavard, J., Marthiens, V., Monnet, C., Lambert, M. and Mege, R. M. (2004). N-cadherin activation substitutes for the cell contact control in cell cycle arrest and myogenic differentiation: involvement of p120 and beta-catenin. *J. Biol. Chem.* **279**, 36795-36802.
- Gluecksohn-Schoenheimer, S. (1949). The effects of a lethal mutation responsible for duplications and twinning in mouse embryos. *J. Exp. Zool.* **110**, 47-76.
- Goichberg, P., Shtutman, M., Ben-Ze'ev, A. and Geiger, B. (2001). Recruitment of beta-catenin to cadherin-mediated intercellular adhesions is involved in myogenic induction. *J. Cell Sci.* **114**, 1309-1319.
- Han, X. H., Jin, Y.-R., Seto, M. and Yoon, J. K. (2011). A WNT/beta-catenin signaling activator, R-spondin, plays positive regulatory roles during skeletal myogenesis. *J. Biol. Chem.* **286**, 10649-10659.
- Jho, E.-H., Zhang, T., Domon, C., Joo, C.-K., Freund, J.-N. and Costantini, F. (2002). Wnt/beta-catenin/Tcf signaling induces the transcription of Axin2, a negative regulator of the signaling pathway. *Mol. Cell Biol.* **22**, 1172-1183.
- Jones, A. E., Price, F. D., Le Grand, F., Soleimani, V. D., Dick, S. A., Megeny, L. A. and Rudnicki, M. A. (2015). Wnt/beta-catenin controls follistatin signalling to regulate satellite cell myogenic potential. *Skeletal Muscle* **5**, 14.
- Krupnik, V. E., Sharp, J. D., Jiang, C., Robison, K., Chickering, T. W., Amaravadi, L., Brown, D. E., Guyot, D., Mays, G., Leiby, K. et al. (1999). Functional and structural diversity of the human Dickkopf gene family. *Gene* **238**, 301-313.
- Kuroda, K., Kuang, S., Taketo, M. M. and Rudnicki, M. A. (2013). Canonical Wnt signaling induces BMP-4 to specify slow myofibrogenesis of fetal myoblasts. *Skeletal Muscle* **3**, 5.
- Le Grand, F., Jones, A. E., Seale, V., Scimè, A. and Rudnicki, M. A. (2009). Wnt7a activates the planar cell polarity pathway to drive the symmetric expansion of satellite stem cells. *Cell Stem Cell* **4**, 535-547.
- Leung, J. Y., Kolligs, F. T., Wu, R., Zhai, Y., Kuick, R., Hanash, S., Cho, K. R. and Fearon, E. R. (2002). Activation of AXIN2 expression by beta-catenin-T cell factor. A feedback repressor pathway regulating Wnt signaling. *J. Biol. Chem.* **277**, 21657-21665.
- Lustig, B., Jerchow, B., Sachs, M., Weiler, S., Pietsch, T., Karsten, U., van de Wetering, M., Clevers, H., Schlag, P. M., Birchmeier, W. et al. (2002). Negative feedback loop of Wnt signaling through upregulation of conductin/axin2 in colorectal and liver tumors. *Mol. Cell Biol.* **22**, 1184-1193.
- MacDonald, B. T., Tamai, K. and He, X. (2009). Wnt/beta-catenin signaling: components, mechanisms, and diseases. *Dev. Cell* **17**, 9-26.
- Martin, B., Schneider, R., Janetzky, S., Waibler, Z., Pandur, P., Köhl, M., Behrens, J., von der Mark, K., Starzinski-Powitz, A. and Wixler, V. (2002). The LIM-only protein FHL2 interacts with beta-catenin and promotes differentiation of mouse myoblasts. *J. Cell Biol.* **159**, 113-122.
- Murphy, M. M., Keefe, A. C., Lawson, J. A., Flygare, S. D., Yandell, M. and Kardon, G. (2014). Transiently active Wnt/beta-catenin signaling is not required but must be silenced for stem cell function during muscle regeneration. *Stem Cell Rep.* **3**, 475-488.
- Pan, D. (2010). The hippo signaling pathway in development and cancer. *Dev. Cell* **19**, 491-505.
- Parisi, A., Lacour, F., Giordani, L., Colnot, S., Maire, P. and Le Grand, F. (2015). APC is required for muscle stem cell proliferation and skeletal muscle tissue repair. *J. Cell Biol.* **210**, 717-726.
- Perry, W. L., III, Vasicek, T. J., Lee, J. J., Rossi, J. M., Zeng, L., Zhang, T., Tilghman, S. M. and Costantini, F. (1995). Phenotypic and molecular analysis of a transgenic insertional allele of the mouse Fused locus. *Genetics* **141**, 321-332.
- Poleskaya, A., Seale, P. and Rudnicki, M. A. (2003). Wnt signaling induces the myogenic specification of resident CD45+ adult stem cells during muscle regeneration. *Cell* **113**, 841-852.
- Rochat, A., Fernandez, A., Vandromme, M., Moles, J.-P., Bouschet, T., Carnac, G. and Lamb, N. J. C. (2004). Insulin and wnt1 pathways cooperate to induce reserve cell activation in differentiation and myotube hypertrophy. *Mol. Biol. Cell* **15**, 4544-4555.
- Rudolf, A., Schirwis, E., Giordani, L., Parisi, A., Lepper, C., Taketo, M. M. and Le Grand, F. (2016). Beta-catenin activation in muscle progenitor cells regulates tissue repair. *Cell Rep.* **15**, 1277-1290.
- Schubert, S. W., Abendroth, A., Kilian, K., Vogler, T., Mayr, B., Knerr, I. and Hashemolhosseini, S. (2008). bZIP-Type transcription factors CREB and OASIS bind and stimulate the promoter of the mammalian transcription factor GCMA/Gcm1 in trophoblast cells. *Nucleic Acids Res.* **36**, 3834-3846.
- Tsika, R. W., Schramm, C., Simmer, G., Fitzsimons, D. P., Moss, R. L. and Ji, J. (2008). Overexpression of TEAD-1 in transgenic mouse striated muscles produces a slower skeletal muscle contractile phenotype. *J. Biol. Chem.* **283**, 36154-36167.
- von Maltzahn, J., Wulf, V., Matern, G. and Willecke, K. (2011). Connexin39 deficient mice display accelerated myogenesis and regeneration of skeletal muscle. *Exp. Cell Res.* **317**, 1169-1178.
- von Maltzahn, J., Chang, N. C., Bentzinger, C. F. and Rudnicki, M. A. (2012). Wnt signaling in myogenesis. *Trends Cell Biol.* **22**, 602-609.
- von Maltzahn, J., Zinoviev, R., Chang, N. C., Bentzinger, C. F. and Rudnicki, M. A. (2013). A truncated Wnt7a retains full biological activity in skeletal muscle. *Nat. Commun.* **4**, 2869.
- Watt, K. I., Turner, B. J., Hagg, A., Zhang, X., Davey, J. R., Qian, H., Beyer, C., Winbanks, C. E., Harvey, K. F. and Gregorevic, P. (2015). The Hippo pathway effector YAP is a critical regulator of skeletal muscle fibre size. *Nat. Commun.* **6**, 6048.
- Yu, H.-M. I., Jerchow, B., Sheu, T.-J., Liu, B., Costantini, F., Puzas, J. E., Birchmeier, W. and Hsu, W. (2005). The role of Axin2 in calvarial morphogenesis and craniosynostosis. *Development* **132**, 1995-2005.
- Zeng, L., Fagotto, F., Zhang, T., Hsu, W., Vasicek, T. J., Perry, W. L., III, Lee, J. J., Tilghman, S. M., Gumbiner, B. M. and Costantini, F. (1997). The mouse Fused locus encodes Axin, an inhibitor of the Wnt signaling pathway that regulates embryonic axis formation. *Cell* **90**, 181-192.
- Zhao, B., Tumaneng, K. and Guan, K.-L. (2011). The Hippo pathway in organ size control, tissue regeneration and stem cell self-renewal. *Nat. Cell Biol.* **13**, 877-883.

## Supplementary Materials and Methods

### *Generation of plasmids*

For knockdowns, shRNA sequences were designed with the software Oligoengine ([www.oligoengine.com](http://www.oligoengine.com)). Plasmids pNLS-GFP (Hashemolhosseini et al., 2000) or pMAX-GFP (Lonza) were used as controls for cell transfections. Mouse Axin1 (NM\_001159598.1), Axin2 (NM\_015732.1),  $\beta$ -catenin (NM\_007614.3) and TEAD1 (NM\_001166584.1) specific complementary oligonucleotides (Table S1) were hybridized and subcloned into pSUPERneoGFP using restriction enzyme sites *HindIII* and *BglII*. Plasmids were transformed in *E.coli* bacteria (NEB 5- $\alpha$ ; New England Biolabs) and extracted from bacteria by alkaline lysis Nucleobond PC100 Midiprep kits (Macherey-Nagel). To assess the knockdown efficiency pSUPERneoGFP plasmid constructs were co-transfected with expression plasmids for N-terminally FLAG-tagged rat Axin1 or mouse Axin2 cDNA (Behrens et al., 1998).

### *Production of recombinant hDkk protein*

Conditioned medium containing recombinant hDkk-1 protein was produced as described before (Krupnik et al., 1999). A full-length human Dkk-1 transcript comprising 801 bp was amplified from a human cDNA library using the oligonucleotides hDkk-1\_BspE1\_fw and hDkk-1\_BamH1\_rev (see Table S1) and cloned into Flag-N2 vector. Serum-free conditioned medium containing soluble Dkk-1 and control medium was collected from 293T cells transiently transfected with hDkk-1-Flag and Flag-N2 alone, respectively, and centrifuged for 10 min with 1.000 g to remove debris.

### *Tissue culture, culturing of primary muscle cells, transfection*

HEK 293 cells were cultured in Dulbecco modified Eagle medium (DMEM) with 10 % FCS. Cells were transfected with 8  $\mu$ g DNA, 400  $\mu$ l DMEM and 30  $\mu$ l of 0,045 % PEI in water



solution. C2C12 cells were maintained for proliferation in DMEM containing 20% (v/v) FCS; for differentiation, the medium was replaced by DMEM with 2% (v/v) heat-inactivated horse serum (HS, Invitrogen). Myotubes were formed after 4–6 days. After isolation primary skeletal muscle cells were seeded on Matrigel-coated plates (Life Technologies) in culture medium (40 % DMEM, 40 % Ham's F10, 20 % FCS, 1 % penicillin/streptomycin, recombinant human fibroblast growth factor (5 ng/ml)). At the time primary skeletal muscle cells reached confluence their medium was replaced for differentiation by 98 % DMEM, 2 % horse serum, and 1 % penicillin/streptomycin. For nucleofections,  $5 \times 10^5$  primary skeletal myoblasts were used according to the manufacturer's instructions (Nucleofector, Lonza). Transfection efficiency was determined after 24 h. At the same time, primary skeletal muscle cells reached confluence and the medium was replaced by differentiation medium (98% DMEM, 2% horse serum, and 1% penicillin/streptomycin).

#### *Generation of Wnt3a-overexpressing C2C12 cells by retroviral infection*

A hemagglutinin-tagged mouse full-length Wnt3a cDNA was excised from pUSE-Wnt3a (Upstate Biotechnology) using PmeI as a restriction enzyme and ligated into pLNCX2 retroviral vector (Clontech). Ecotropic Phoenix retroviral packaging cells were cultured in 10 cm dishes and transfected with 5  $\mu$ g pLNCX2-Wnt3a retroviral vector and 10  $\mu$ l polyethylenimine (1 mg/ml). Supernatant was collected 24 h later and centrifuged for 5 min with 1.000 g to remove debris. Supernatant was supplemented with 4  $\mu$ g/ml polybrene, distributed on recipient C2C12 cells and spinoculated for 1 h with 2.300 g at 33 °C. Recipient C2C12 cells were cultured for another 48 h and then subjected to selection for neomycin resistance indicating stable integration of the retroviral construct.

### *In situ hybridization*

Cells were fixed in 4% PFA overnight, dehydrated in 25% to 100% methanol solutions for 5 minutes each, and stored at -20°C. To perform *in situ* hybridization cells were rehydrated, quickly washed in PBST and treated for 15min with Proteinase K (20µg/ml). After refixation in 0.2% glutaraldehyde in 4% PFA, cells were washed, incubated for 2h in pre-hybridization buffer and hybridized overnight at 55°C with corresponding denatured ( 5min 95°C, followed by 3min on ice) riboprobes (10µl/mL). For generation of antisense probes both plasmids were linearized with *NdeI* and antisense riboprobes were made using T7 polymerase. Sense riboprobes were generated by restriction digestion of the Axin 1 cDNA-containing plasmid with *SacII* and the Axin2 cDNA-containing plasmid with *NcoI* and using the SP6 polymerase. Next day cells were washed, blocked with 10% FCS in TBST and incubated for 4h with a 1:2.000 dilution of the anti-Digoxigenin-AP antibody (11093274910, Roche Diagnostics) in 1% FCS in TBST. After six washing steps, cells were kept in TBST overnight. Next day cells were equilibrated in NTM solution (0.1M Tris, pH 9.5, 0.5M NaCl, 0.05M MgCl<sub>2</sub>, 0.1% Tween 20) and developed with 90 mM NBT (11383213001, Roche Diagnostics) and 110mM BCIP (11383221001, Roche Diagnostics) in NTM solution.

### *Protein lysates, antibodies and Western Blot analysis*

At indicated time points cells were lysed for 20 min on ice either in 100 µl of hypotonic buffer (25 mM Tris-HCl pH 8.0, 1 mM EDTA, 1 mM phenylmethylsulfonyl fluoride) to obtain the cytosolic fractions for the analysis of β-catenin or in L1 lysis buffer (20 mM Tris-HCl pH 7.4, 150 mM NaCl, 1 mM EDTA, 1% Triton X-100, 1 mM dithiothreitol, 1 mM phenylmethylsulfonyl fluoride) for the analysis of Axin2. Diaphragm and tibialis anterior muscles were lysed in L1 lysis buffer for analysis of β-galactosidase expression. Protein concentrations were determined by the Bradford protein assay (Bio-Rad).

After Western blot transfer, membranes were blocked in 5 % BSA or 5 % non-fat dry milk in PBS or TBS, 0.1 % Tween20 (Carl Roth) for 1 h at room temperature. Following antibodies were used in immunoblotting experiments: Axin1 (C76H11, Cell Signaling Technology), Axin2 (ab32197, Abcam, or 1:100 dilution of hybridoma supernatant, mouse C/G7),  $\beta$ -catenin (1:400, Transduction Laboratories (Lustig et al., 2002) or 1:3.000, (6B3), Cell Signaling Technology),  $\beta$ -galactosidase (1:3.000, A11132, Molecular Probes), GAPDH (1:3.000, sc-25778, Santa Cruz Biotechnology Inc.). HRP-conjugated secondary antibodies were used at 1:3.000 dilution.

For the chemiluminescence reaction 3 ml of 0,25 mg/ml Luminol (A-4685, Sigma Aldrich Chemie) in 0.1 M Tris pH 8.6 solution and 40  $\mu$ l of 1,1 mg/ml Para-hydroxy-Cumarinic acid (C-9008, Sigma Aldrich Chemie) in DMSO were mixed with 3 ml of PBS and 1.2  $\mu$ l of 30 % H<sub>2</sub>O<sub>2</sub>. For densitometric analysis in ImageJ the background was subtracted with rolling ball function with a 1.000 pixels radius and disabled smoothing option. Then protein bands of interest were labeled and measured.

#### *Tissue sections, histochemical stainings, immunohistochemistry*

Muscles were cryotome-sectioned (10  $\mu$ m) and used either for histochemical or immunofluorescence stainings. After staining sections were embedded in DPX; mowiol or Permafluor (Thermo Fisher Scientific). Hematoxylin & Eosin staining: sections were incubated for 5 minutes in Mayer's Hemalaun solution (Merck), washed in tap water for 15 minutes, dipped in a 4% HCl acidic ethanol solution, washed again for 10 minutes in tap water, then immersed in Eosin solution (Merck) for 10 minutes and dehydrated in 50 to 100% ethanol solutions for 1 minute each. Modified Gomori trichrome staining: sections were incubated in Shandon Hematoxyline (Fisher Scientific) for 15 minutes, washed in tap water for 15 minutes, then incubated in Gomori solution (Sigma-Aldrich Chemie) for 15 minutes again, afterwards washed in tap water and incubated in 100 % ethanol. Nicotinamide adenine dinucleotid (NADH) staining: sections were incubated for 30 minutes at 37°C in a solution containing NBT (Sigma-Aldrich

Chemie), 50 mM Tris/HCl and NADH (Sigma-Aldrich Chemie), then washed in distilled water and mounted. X-Gal staining: muscle cross-sections or single myofibers were fixed in 1% PFA for 5 minutes, whole muscles were fixed for 1 hour, and after 3 washes of 5 minutes in PBS were incubated in X-Gal staining solution at 37°C, consisting of 0,75mg/ml X-Gal, 5mM potassium ferricyanide, 5mM potassium ferrocyanide, 0,01% sodium deoxycholate, 0,02% NP-40, 2mM magnesium chloride and 20mM Tris in phosphate buffered saline. Muscle cross-sections of CTX-treated and control animals were fixed in 2%PFA and X-Gal stained with the  $\beta$ -Gal staining set ( $\beta$ -Gal staining set, Roche) at 37°C for 72 hours before immunofluorescence staining. Stained muscle tissues were visualized using the Zeiss Discovery V8 stereo microscope equipped with an AxioCam HRm camera and the Zeiss AxioVision software Release 4.8 (Carl Zeiss MicroImaging). For NMJ visualization fiber bundles were pulled from X-Gal stained EDL muscles and incubated with Rhodamin-conjugated  $\alpha$ -bungarotoxin (1:2.500 dilution, Rh-BTX, Thermo Fischer Scientific). After 3 washes fiber bundles were embedded in mowiol and visualized with a 63-fold objective (Zeiss Examiner E1).

#### *Immunofluorescence staining, fluorescence microscopy, morphometry*

Following antibodies from the DSHB were used for staining of myosin heavy chain expression at indicated dilutions:  $\alpha$ - and  $\beta$ -slow myosin heavy chain (BA-D5, 1:1.000), myosin heavy chain type 2A (SC-71, 1:1.000), myosin heavy chain type 2B (BF-F3, 1:500), mouse anti-MHCdev (F1.652). Further the rabbit anti- $\beta$ -catenin antibody (#9582, Cell Signaling, 1:500), rabbit anti-TEAD1 (D9X2L, Cell Signaling, 1:2.000), rabbit anti-YAP/TAZ (D2E4, Cell Signaling, 1:500), mouse anti-Pax7 hybridoma supernatant (Developmental Studies Hybridoma Bank [DSHB], undiluted), rabbit anti-Ki-67 (Rb1510-P0, Thermo Fisher Scientific, 1:500), rabbit anti-MyoD (C20, Santa Cruz Biotechnology Inc., 1:200), chicken anti-laminin (LS-C96142, LifeSpanBioSciences, 1:1.000) and rabbit anti-laminin (L9393, Sigma-Aldrich, 1:1000) antibodies were used. Secondary antibodies conjugated to Alexa488, Alexa 546, Cy3 (Dianova)

or Alexa647-conjugated dyes were used for detection. IgG1 specific secondary antibodies, coupled to Cy3 dye were used for detection of Pax7.

For fluorescence microscopy, stained cross-sections or single myofibers were analyzed and documented using the Zeiss Axio Examiner Z1 microscope equipped with an AxioCam MRm camera and the Zeiss AxioVision software Release 4.8 (Carl Zeiss MicroImaging). Images of CTX treated or control muscle cross-sections were taken with the Axio Observer microscope (Carl Zeiss MicroImaging).

To assess fiber type specificity of X-Gal positive fibers and fiber type distribution, images of whole plantaris EDL and TA muscles area on hindlimb cross sections were acquired using a 5-fold objective. For quantification of YAP/TAZ, TEAD1 and  $\beta$ -catenin expression images of corresponding areas were acquired as z-stacks with a 20-fold objective. X-Gal positive and negative fibers were determined using adjacent cross sections, that were stained with X-Gal. Image processing and quantification were performed with the Cell Counter plugin in ImageJ (NIH). The cross-sectional area of muscle fibers was quantified using the AxioVision Software Release 4.8 (Carl Zeiss MicroImaging).

#### *TUNEL assay*

TUNEL assays were performed with the ApopTag® Red In Situ Apoptosis Detection Kit (Merck). Muscle cross sections were permeabilized with 0.5 % Triton/PBS, incubated in a solution of ethanol/acetic acid (2:1) for 5 minutes at -20°C, incubated for 10 seconds with equilibration buffer, then for 1 hour at 37°C with the TdT Enzyme, and the reaction was then stopped with the Stop/Wash Buffer. Finally, the muscle cross sections were incubated overnight at 4°C with the Anti-Digoxigenin-Rhodamine conjugate. Next day muscle cross sections were washed, stained with DAPI and mounted with Mowiol.

## Supplementary references

- Behrens, J., Jerchow, B. A., Wurtele, M., Grimm, J., Asbrand, C., Wirtz, R., Kuhl, M., Wedlich, D. and Birchmeier, W.** (1998). Functional interaction of an axin homolog, conductin, with beta-catenin, APC, and GSK3beta. *Science* **280**, 596-599.
- Hashemolhosseini, S., Moore, C., Landmann, L., Sander, A., Schwarz, H., Witzemann, V., Sakmann, B. and Brenner, H. R.** (2000). Electrical activity and postsynapse formation in adult muscle: gamma-AChRs are not required. *Mol Cell Neurosci* **16**, 697-707.
- Krupnik, V. E., Sharp, J. D., Jiang, C., Robison, K., Chickering, T. W., Amaravadi, L., Brown, D. E., Guyot, D., Mays, G., Leiby, K., et al.** (1999). Functional and structural diversity of the human Dickkopf gene family. *Gene* **238**, 301-313.
- Lustig, B., Jerchow, B., Sachs, M., Weiler, S., Pietsch, T., Karsten, U., van de Wetering, M., Clevers, H., Schlag, P. M., Birchmeier, W., et al.** (2002). Negative feedback loop of Wnt signaling through upregulation of conductin/axin2 in colorectal and liver tumors. *Mol Cell Biol* **22**, 1184-1193.

**Table S1. Oligonucleotides**

Axin1 shRNA4-fwd	GATCCCCGCACTTACCGAATGCCAAAGGTTCAAGAGACCTTTGGCATTCCGGTAAGTGCTTTTTA
Axin1 shRNA4-rev	AGCTTAAAAAGCACTTACCGAATGCCAAAGGTTCTTGAACCTTTGGCATTCCGGTAAGTGCGGG
Axin2 shRNA5-fwd	GATCCCCGAAGGCGAGTGACGAATTTGCTTCAAGAGAGCAAATTCGTCACCTCGCCTTCTTTTTA
Axin2 shRNA5-rev	AGCTTAAAAAGAAGGCGAGTGACGAATTTGCTTCTTGAAGCAAATTCGTCACCTCGCCTTCGGG
Axin1-riboprobe-fwd	ATAGCGGCCGCATGCAGAGTCCCAAATGAATGTCCAGGAG
Axin1-riboprobe-rev	ATAGCGGCCGCCCTCTGCTTGGAGGGCAGTTTGTCTTCT
Axin2-riboprobe-fwd	ATAACTAGTATGAGTAGCGCCGTGTTAGTGACTCTCCTT
Axin2-riboprobe-rev	ATACTCGAGTTGAGCCTTCAGCATCCTCCTGTATGGAAT
Axin1-qPCR-fwd	TGCAGTGGATCATTGAGGGAG
Axin1-qPCR-rev	TTTGTCTCTGCTTGGAGGG
Axin2-qPCR-fwd	GACGGACAGTAGCGTAGATGG
Axin2-qPCR-rev	GGTCTCTTCATAGCTGCC
RPL8-qPCR-fwd	GTTCTGTACTGCGGCAAGA
RPL8-qPCR-rev	ACAGGATTCATGGCCACACC
CTGF-qPCR-fwd	CTAGCTGCCTACCGACTGGAA
CTGF-qPCR-rev	CAAACCTGACAGGCTTGGCG
Ankrd1-qPCR-fwd	TGGAGGAAACGCAGATGTCC
Ankrd1-qPCR-rev	TCCCAGCACAGTTCTTGACC
Cyr61-qPCR-fwd	AAGAGGCTTCCTGTCTTTGGC
Cyr61-qPCR-rev	ATCGGAACCGCATCTTCAACA
hDkk1_BspE1_fw	TCCCTCCGGAATGGCTCTGGGCGCAGC
hDkk1_BamH1_rev	GCGGGATCCGTGTCTCTGACAAGTGTGAAGCCTAG
Cat5-7	GATCCCCGCACACGAATGGATCACAAGATTCAAGAGATCTTGTGATCCATTCCGTGTGCTTTTTA
Cat5-8	AGCTTAAAAAGCACACGAATGGATCACAAGATCTTGAATCTTGTGATCCATTCCGTGTGCGGG
Cat5-11	GATCCCCGCTACAGCAATTTCTGATTTCTTCAAGAGAGAAATCAGAAATTCGCTGTAGCTTTTTA
Cat5-12	AGCTTAAAAAGTTATCAAACCTAGCCTTCTTCTTGAAGAAGGCTAGGGTTTGATAACGGG
TEAD1-7	GATCCCCGGAAGAACTTGTCATCAACCTTCAAGAGAGGTTGATGACAAGTTTCTTCCTTTTA
TEAD1-8	AGCTTAAAAAGGAAGAACTTGTCATCAACCTTCTTGAAGGTTGATGACAAGTTTCTTCCGGG